## Supplementary Note 1: Data preprocessing

The preprocessing process of CT images is shown in Supplementary Fig.6. Firstly, a physician identifies the rectangular region of interest (ROI) in the original CT images and performs cropping. The rectangular ROI encloses the contour of the entire uterus. Subsequently, the ROI image is adjusted to a $224\times224$ square.

**Supplementary Note 2: robust feature transfer networks**

This study constructs two robust feature transfer (RFT) networks to achieve robust feature transfer from VFM to CNN. Based on equation (1), the representation difference between VFM and CNN for the same data is measured. By minimizing this term, the learning process of CNN to capture the representation from VFM is constrained:

$$L_2 = \left\| r_\theta (C_\theta^n (x)) - V^m (x) \right\|_2^2 \tag{1}$$

where, $(m, n) \in \partial$ , $\partial$ is the predefined set of model layer matches, where the total number of matched pairs is denoted as *P*. $V^m(x)$ represents the intermediate feature map of the *m*th model layer in the VFM, while $C_{\theta_k}^n(x)$ represents the intermediate feature map of the *n*th model layer in the CNN model *k*. $r_{\theta_k}$ is a linear transformation parameterized by $\theta_k$ for point-wise convolutions, ensuring that the number of feature maps between the two models is consistent. Additionally, this parameter is only updated and used during the training of the target domain model, forming the target model parameters $\theta_k$ along with $C_{\theta_k}$. $x$ and $y$ represent the input data and true labels, respectively.

Each convolutional layer of the CNN consists of multiple convolutional kernels. The CNN extracts data features through these convolutional kernels, with each kernel generating an intermediate feature map. After linear transformation, these intermediate feature maps are matched one by one with the intermediate feature maps generated by the transformer block of VFM, forming the feature transfer channels. We employ RFT network1 $\phi_k$ to calculate the weights $\omega_c^{m,n}$ for each feature transfer channel. The structure of RFT network 1 consists of *P* sets of fully connected layers, pooling layers, and a softmax layer. This network takes the features from the VFM as input and produces the output through the softmax layer. In the equation (2), $\omega_c^{m,n}$ is a learnable parameter that facilitates the matching of the *m*th layer feature from the VFM with the *n*th layer feature from the CNN model.

$$\omega_c^{m,n} = f_{\phi_k}^{m,n}(V^m(x)) \tag{2}$$

Then, we employ RFT network 2 to calculate the weights $\lambda_k^{m,n}$ for model layer matching. The structure of RFT network 2 consists of *P* sets of fully connected layers, pooling layers, and a

ReLU6 layer, forming a fully connected network. This network takes the features from the VFM as input and produces the output through the ReLU6 activation layer.

$$\lambda_k^{m,n} = g_{\phi_k}^{m,n}(V^m(x)) \tag{3}$$

where, $\lambda_k^{m,n} > 0$, and the initial value is 1.0. RFT networks $\phi_k$ are updated based on the change in loss of the CNN network, and the details are illustrated in Algorithm 1.

**Supplementary Note 3: The construction of VFMGL robustness critical layers**

By combining equations (1) and (2), the feature channel transfer loss (4) can be obtained.

$$L_{\text{wfm}}^{m,n}(\theta_k \mid x, \omega^{m,n}) = \frac{1}{HW}\sum\nolimits_c \omega_c^{m,n} \sum\nolimits_{i,j} (r_{\theta_k}(C_{\theta_k}^n(x))_{c,i,j} - V^m(x)_{c,i,j})^2 \tag{4}$$

where, $H \times W$ represents the size of the output feature maps from $(r_{\theta_k}(C_{\theta_k}^n(x))$ and $V^m(x)$.

In combination with formula (3), knowledge transfer total loss as follows:

$$L_{\text{wfm}}^{m,n}(\theta_k \mid x, \phi_k) = \sum\nolimits_{(m,n\in\partial)} \lambda_k^{m,n} L_{\text{wfm}}^{m,n}(\theta_k \mid x, \omega^{m,n}) \tag{5}$$

VFMGL's total training loss in Stage I is shown in Equation (6), where $L_{\text{org}}$ represents the local model's standard cross-entropy loss(the segmentation task employs the dice loss). The VFMGL training process is visible in Algorithm 1.

$$L_{\text{stageI}}(\theta_k \mid x, y, \phi_k) = L_{\text{wfm}}^{m,n}(\theta_k \mid x, \phi_k) + L_{\text{org}}(\theta_k \mid x, y) \tag{6}$$

Algorithm 1

Input: the number of communication rounds $n$, the number of centers $K$, the number of training rounds for the local model $E$, the number of internal cycles of knowledge transfer $N$, and the learning rate $\alpha$, the number of randomly sampled data batches $B$, Data batch selection threshold $TV$.

Output: Local model parameters $\theta_1 \dots \theta_k \dots \theta_K$ .

1. Initialize the model parameters $\theta_k$ , load the VFM pre-trained model parameters
2. For $i$=1 to $n$ do
3.  For $k$=1 to $K$ do
4.   For $e$=1 to $E$ do
5.    For $j$=1 to $N$ do
6.     $\theta_k \leftarrow \theta_k - a\nabla_\theta L_{\text{wfm}}(\theta_k \mid x, \phi_k)$
7.     $\theta_k \leftarrow \theta_k - a\nabla_\theta L_{\text{org}}(\theta_k \mid x, y)$
8.     $\phi_k \leftarrow \phi_k - a\nabla_\phi L_{\text{org}}(\theta_k \mid x, y)$
9.    Return $\theta_k$
10.    Compute $L$
11.    If $i$=1:
12.     Medical center sends $\theta_k$ to the server
13.     Aggregate shared model $\theta_{shared} \leftarrow \frac{\sum_{k=1}^{K}\theta_k}{K}$
14.     Server sends $\theta_{shared}$ to each medical center
15.    Else:
16.     For $b$ in $B$ do
17.      Batch_data=random_select(data)
18.      Compute $KL$ with batch data
19.      If $KL/L<TV$:
20.       $\theta_k \leftarrow \theta_k - a\nabla_\theta L_{\text{stageII}}(\theta_k \mid x, y)$
21.     Return $\theta_k$
22.     Medical center sends $\theta_k$ to the server for aggregation of the shared model
23. End

**Supplementary Note 4: DDBL**

In a multi-center setting with distributional heterogeneity, it is possible that some data possess better commonality. Based on this assumption, we have constructed a straightforward data deduction framework to identify local data that better aligns with the global data distribution for local model training. In FL, each center has access to both the globally distributed model parameters sent by the server and the locally trained model parameters. By randomly sampling a batch and feeding it into both the shared and local models simultaneously, we input the feature maps from the last model layer (before the Avgpool layer) of both models into the classification layer of the shared model, generating two sets of predicted probability distributions(For segmentation models, the feature maps of the last encoding layer of the model are inputted into the decoding layer of the shared model.). We then compute the Kullback-Leibler(KL) divergence based on equation (7). Simultaneously, by utilizing the predicted probability distribution of the local model and the true label distribution, we calculate the distribution discrepancy based on equation (8).

$$KL = -\sum_i Q_1(i)\log\left(\frac{Q_1(i)}{Q_2(i)}\right) \tag{7}$$

$$L = -\sum_i P(i)\log(Q_3(i)) \tag{8}$$

In the above equations, $Q_1$ represents the predicted probability distribution output by the shared model based on the local model representation, $Q_2$ represents the predicted probability distribution output by the shared model based on its own representation, and $P$ represents the true label distribution. $i$ denotes the index of the category. $Q_3$ represents the probability distribution of predictions based on the outputs of the local model's representations.

We use $KL/L$ to measure the heterogeneity of batch data. With the iteration of local model training, for data with small heterogeneity, both the $L$ value and $KL$ value will continuously decrease. On the other hand, for data with strong heterogeneity, the $KL$ value will be challenging to reduce, while the $L$ value will decrease rapidly. Therefore, we set a threshold ($TV$, default value 4) to filter out batches of data with significant heterogeneity. The details are illustrated in Algorithm 1.

## Supplementary Note 5: The training strategy via DDBL

This study constructs the knowledge distillation loss function for the second stage of VFMGL based on KL divergence (Equation (9)). After freezing the robustness critical layer obtained in Stage I, the remaining model layers of the local model are constrained to acquire multi-center knowledge from the shared model.

$$L_{\mathrm{KL}}(\theta_k \mid z_1, z_2) = \sum_i \left(\log\left(\frac{\exp(z_1(i)/temp)/\sum_j \exp(z_1(j)/temp)}{\exp(z_2(i)/temp)/\sum_j \exp(z_2(j)/temp)}\right) \bullet \frac{\exp(z_1(i)/temp)}{\sum_j \exp(z_1(j)/temp)}\right) \quad (9)$$

Where, $z_1$ and $z_2$ are probability distributions calculated by the shared model classification head based on the representations generated by the local model and the shared model for the same sample, respectively. $z_1(i)$ and $z_2(i)$ represent the probabilities of the *i*th sample for each distribution. Here, *i* represents a category in the predicted distribution, and *j* represents the index of all categories. Hyper-parameter *temp* is used to control the smoothness of the probability distribution.

Combining Equation (9) with the standard cross-entropy $L_{\mathrm{org}}$, the total loss function for Stage II is given by Equation (10).

$$L_{\mathrm{stageII}}(\theta_k \mid x, y) = (1-\beta) \bullet L_{\mathrm{KL}}(\theta_k \mid z_1, z_2) + \beta L_{\mathrm{org}}(\theta_k \mid x, y) \quad (10)$$

Where $\beta$ is a hyper-parameter between 0 and 1, used to balance the relative importance of the two loss terms, with a default value of 0.5.

## Supplementary Note 6: Adaptive knowledge and common knowledge of VFMGL

The analysis of adaptive knowledge and common knowledge in VFMGL involves two main steps. Initially, local models from each center extract features from the test and train datasets of all centers. Following this, the extracted features undergo a round of Max-Relevance and Min-Redundancy (mRMR) feature selection to identify 256 deep learning (DL) features. Subsequently, the DL features are categorized into two groups based on NMI and MI to eliminate differences between categories. A correlation analysis is then performed on the DL features of NMI and MI, and a correlation heat map is constructed. From this analysis, features exhibiting the highest correlation within the same center and the lowest correlation across different data centers are identified as adaptive knowledge. Conversely, features displaying the highest correlation across different data centers are considered common knowledge.

## Supplementary Note 7: Classifier

For classification tasks, VFMGL is not limited to specific classification layers or classifiers. For small-sample datasets, to enhance the utilization of model features, each data center can utilize the convolutional kernels of its own local model as feature extractors. Multiple feature maps are extracted from the local image data of each patient in the local dataset. Subsequently, the average value of each feature map is computed to obtain a set of unified DL features. Finally, sparse Bayesian extreme learning machines [1] are used to construct the prediction labels (Supplementary Fig.7).

**Supplementary Table 1. Comparison of the performance of six methods in use case 1**

| Center | Methods | AUC | Sensitivity | Specificity | Accuracy | PPV | NPV | F1 |
|---|---|---|---|---|---|---|---|---|
| A | FedAvg | 0.676 | 0.461(111/241) | 0.794(27/34) | 0.502(138/275) | 0.941(111/118) | 0.172(27/157) | 0.619 |
| | FedProx | 0.702 | 0.448(108/241) | 0.824(28/34) | 0.495(136/275) | 0.947(108/114) | 0.174(28/161) | 0.608 |
| | HarmoFL | 0.719 | 0.685(165/241) | 0.647(22/34) | 0.680(187/275) | 0.932(165/177) | 0.224(22/98) | 0.790 |
| | MetaFed | 0.732 | 0.705(170/241) | 0.647(22/34) | 0.698(192/275) | 0.934(170/182) | 0.237(22/93) | 0.804 |
| | Virchow | 0.716 | 0.622(150/241) | 0.706(24/34) | 0.633(174/275) | 0.938(150/160) | 0.209(24/115) | 0.748 |
| | VFMGL | 0.798 | 0.884(213/241) | 0.500(17/34) | 0.836(230/275) | 0.926(213/230) | 0.378(17/45) | 0.905 |
| B | FedAvg | 0.710 | 0.696(16/23) | 0.500(3/6) | 0.655(19/29) | 0.842(16/19) | 0.300(3/10) | 0.762 |
| | FedProx | 0.754 | 0.739(17/23) | 0.667(4/6) | 0.724(21/29) | 0.895(17/19) | 0.400(4/10) | 0.810 |
| | HarmoFL | 0.790 | 0.739(17/23) | 0.667(4/6) | 0.724(21/29) | 0.895(17/19) | 0.400(4/10) | 0.810 |
| | MetaFed | 0.775 | 0.609(14/23) | 0.667(4/6) | 0.621(18/29) | 0.875(14/16) | 0.308(4/13) | 0.718 |
| | Virchow | 0.804 | 0.826(19/23) | 0.667(4/6) | 0.793(23/29) | 0.905(19/21) | 0.500(4/8) | 0.864 |
| | VFMGL | 0.833 | 0.565(13/23) | 0.833(5/6) | 0.621(18/29) | 0.929(13/14) | 0.333(5/15) | 0.703 |
| C | FedAvg | 0.643 | 0.571(8/14) | 1.000(1/1) | 0.600(9/15) | 1.000(8/8) | 0.143(1/7) | 0.727 |
| | FedProx | 0.714 | 0.714(10/14) | 0.000(0/1) | 0.667(10/15) | 0.909(10/11) | 0.000(0/4) | 0.800 |
| | HarmoFL | 0.786 | 0.929(13/14) | 0.000(0/1) | 0.867(13/15) | 0.929(13/14) | 0.000(0/1) | 0.929 |
| | MetaFed | 0.786 | 0.786(11/14) | 1.000(1/1) | 0.800(12/15) | 1.000(11/11) | 0.250(1/4) | 0.880 |
| | Virchow | 0.786 | 0.857(12/14) | 0.000(0/1) | 0.800(12/15) | 0.923(12/13) | 0.000(0/2) | 0.889 |
| | VFMGL | 0.857 | 0.857(12/14) | 0.000(0/1) | 0.800(12/15) | 0.923(12/13) | 0.000(0/2) | 0.889 |
| D | FedAvg | 0.765 | 0.882(97/110) | 0.500(4/8) | 0.856(101/118) | 0.960(97/101) | 0.235(4/17) | 0.919 |
| | FedProx | 0.752 | 0.500(55/110) | 1.000(8/8) | 0.534(63/118) | 1.000(55/55) | 0.127(8/63) | 0.667 |
| | HarmoFL | 0.805 | 0.582(64/110) | 0.875(7/8) | 0.602(71/118) | 0.985(64/65) | 0.132(7/53) | 0.732 |
| | MetaFed | 0.807 | 0.836(92/110) | 0.500(4/8) | 0.814(96/118) | 0.958(92/96) | 0.182(4/22) | 0.893 |
| | Virchow | 0.823 | 0.636(70/110) | 0.875(7/8) | 0.653(77/118) | 0.986(70/71) | 0.149(7/47) | 0.773 |
| | VFMGL | 0.848 | 0.745(82/110) | 0.875(7/8) | 0.754(89/118) | 0.988(82/83) | 0.200(7/35) | 0.849 |

Notes: VFMGL, Vision Foundation Model General Lightweight; AUC, Area Under the Curve; PPV, Positive Predictive Value; NPV, Negative Predictive Value. Source data are provided as a Source Data file.

**Supplementary Table 2. Comparison of the performance of six methods in use case 2**

| Center | Methods | AUC | Sensitivity | Specificity | Accuracy | PPV | NPV | F1 |
|---|---|---|---|---|---|---|---|---|
| A | FedAvg | 0.9358 | 0.8484 (5043/5944) | 0.9561 (5683/5944) | 0.9023 (10726/11888) | 0.9508 (5043/5304) | 0.8632 (5683/6584) | 0.8967 |
| | FedProx | 0.9875 | 0.9263 (5506/5944) | 0.9739 (5789/5944) | 0.9501 (11295/11888) | 0.9726 (5506/5661) | 0.9297 (5789/6227) | 0.9489 |
| | HarmoFL | 0.9863 | 0.9127 (5425/5944) | 0.9754 (5798/5944) | 0.9441 (11223/11888) | 0.9738 (5425/5571) | 0.9178 (5798/6317) | 0.9423 |
| | MetaFed | 0.9874 | 0.9268 (5509/5944) | 0.9798 (5824/5944) | 0.9533 (11333/11888) | 0.9787 (5509/5629) | 0.9305 (5824/6259) | 0.9520 |
| | Virchow | 0.9831 | 0.9633 (5726/5944) | 0.9680 (5754/5944) | 0.9657 (11480/11888) | 0.9679 (5726/5916) | 0.9635 (5754/5972) | 0.9656 |
| | VFMGL | 0.9992 | 0.9882 (5874/5944) | 0.9896 (5882/5944) | 0.9889 (11756/11888) | 0.9896 (5874/5936) | 0.9882 (5882/5952) | 0.9889 |
| B | FedAvg | 0.8420 | 0.7946 (2773/3490) | 0.8479 (2960/3491) | 0.8212 (5733/6981) | 0.8393 (2773/3304) | 0.8050 (2960/3677) | 0.8163 |
| | FedProx | 0.9711 | 0.9060 (3162/3490) | 0.9215 (3217/3491) | 0.9138 (6379/6981) | 0.9203 (3162/3436) | 0.9075 (3217/3545) | 0.9131 |
| | HarmoFL | 0.9658 | 0.8837 (3084/3490) | 0.9184 (3206/3491) | 0.9010 (6290/6981) | 0.9154 (3084/3369) | 0.8876 (3206/3612) | 0.8993 |
| | MetaFed | 0.9776 | 0.9095 (3174/3490) | 0.9433 (3293/3491) | 0.9264 (6467/6981) | 0.9413 (3174/3372) | 0.9124 (3293/3609) | 0.9251 |
| | Virchow | 0.9795 | 0.8123 (2835/3490) | 0.9989 (3487/3491) | 0.9056 (6322/6981) | 0.9986 (2835/2839) | 0.8419 (3487/4142) | 0.8959 |
| | VFMGL | 0.9973 | 0.9481 (3309/3490) | 0.9974 (3482/3491) | 0.9728 (6791/6981) | 0.9973 (3309/3318) | 0.9506 (3482/3663) | 0.9721 |
| C | FedAvg | 0.9713 | 0.9155 (7787/8506) | 0.9509 (8087/8505) | 0.9332 (15874/17011) | 0.9491 (7787/8205) | 0.9184 (8087/8806) | 0.9320 |
| | FedProx | 0.9892 | 0.9474 (8059/8506) | 0.9714 (8262/8505) | 0.9594 (16321/17011) | 0.9707 (8059/8302) | 0.9487 (8262/8709) | 0.9589 |
| | HarmoFL | 0.9829 | 0.9319 (7927/8506) | 0.9566 (8136/8505) | 0.9443 (16063/17011) | 0.9555 (7927/8296) | 0.9336 (8136/8715) | 0.9436 |
| | MetaFed | 0.9886 | 0.9452 (8040/8506) | 0.9688 (8240/8505) | 0.9570 (16280/17011) | 0.9681 (8040/8305) | 0.9465 (8240/8706) | 0.9565 |
| | Virchow | 0.9670 | 0.8594 (7310/8506) | 0.9805 (8339/8505) | 0.9199 (15649/17011) | 0.9778 (7310/7476) | 0.8746 (8339/9535) | 0.9148 |
| | VFMGL | 0.9995 | 0.9911 (8430/8506) | 0.9915 (8433/8505) | 0.9913 (16863/17011) | 0.9915 (8430/8502) | 0.9911 (8433/8509) | 0.9913 |
| D | FedAvg | 0.9763 | 0.9067 (11772/12984) | 0.9546 (12394/12984) | 0.9306 (24166/25968) | 0.9523 (11772/12362) | 0.9109 (12394/13606) | 0.9289 |
| | FedProx | 0.9925 | 0.9478 (12306/12984) | 0.9784 (12704/12984) | 0.9631 (25010/25968) | 0.9778 (12306/12586) | 0.9493 (12704/13382) | 0.9626 |
| | HarmoFL | 0.9856 | 0.9216 (11966/12984) | 0.9718 (12618/12984) | 0.9467 (24584/25968) | 0.9703 (11966/12332) | 0.9253 (12618/13636) | 0.9453 |
| | MetaFed | 0.9927 | 0.9477 (12305/12984) | 0.9823 (12754/12984) | 0.9650 (25059/25968) | 0.9817 (12305/12535) | 0.9495 (12754/13433) | 0.9644 |
| | Virchow | 0.9736 | 0.6842 (8883/12984) | 0.9992 (12973/12984) | 0.8417 (21856/25968) | 0.9988 (8883/8894) | 0.7598 (12973/17074) | 0.8120 |
| | VFMGL | 0.9977 | 0.9427 (12240/12984) | 0.9988 (12969/12984) | 0.9708 (25209/25968) | 0.9988 (12240/12255) | 0.9457 (12969/13713) | 0.9699 |
| E | FedAvg | 0.9827 | 0.9439 (13849/14672) | 0.9567 (14038/14673) | 0.9503 (27887/29345) | 0.9562 (13849/14484) | 0.9446 (14038/14861) | 0.9500 |
| | FedProx | 0.9946 | 0.9600 (14085/14672) | 0.9808 (14392/14673) | 0.9704 (28477/29345) | 0.9804 (14085/14366) | 0.9608 (14392/14979) | 0.9701 |
| | HarmoFL | 0.9912 | 0.9624 (14121/14672) | 0.9554 (14019/14673) | 0.9589 (28140/29345) | 0.9557 (14121/14775) | 0.9622 (14019/14570) | 0.9590 |
| | MetaFed | 0.9947 | 0.9625 (14122/14672) | 0.9761 (14322/14673) | 0.9693 (28444/29345) | 0.9757 (14122/14473) | 0.9630 (14322/14872) | 0.9691 |
| | Virchow | 0.9589 | 0.8676 (12729/14672) | 0.9826 (14417/14673) | 0.9251 (27146/29345) | 0.9803 (12729/12985) | 0.8812 (14417/16360) | 0.9205 |
| | VFMGL | 0.9993 | 0.9845 (14445/14672) | 0.9922 (14559/14673) | 0.9884 (29004/29345) | 0.9922 (14445/14559) | 0.9846 (14559/14786) | 0.9883 |

Notes: VFMGL, Vision Foundation Model General Lightweight; AUC, Area Under the Curve; PPV, Positive Predictive Value; NPV, Negative Predictive Value. Source data are provided as a Source Data file.

**Supplementary Table 3. Comparison of the performance of six methods in use case 3**

| Center | Methods | Dice | ASSD | Sensitivity | Specificity | PPV | IOU | F1 |
|---|---|---|---|---|---|---|---|---|
| A | FedAvg | 0.5183 | 55.6626 | 0.7629 | 0.7337 | 0.1240 | 0.1186 | 0.2133 |
| | FedProx | 0.8268 | 23.4177 | 0.6776 | 0.9894 | 0.7460 | 0.5468 | 0.7102 |
| | HarmoFL | 0.9253 | 6.7873 | 0.8624 | 0.9951 | 0.8711 | 0.7481 | 0.8667 |
| | MetaFed | 0.7531 | 23.1151 | 0.5629 | 0.9897 | 0.7364 | 0.4758 | 0.6381 |
| | MedSAM | 0.9163 | 5.3587 | 0.7665 | 0.9989 | 0.9682 | 0.7399 | 0.8556 |
| | VFMGL | 0.9340 | 5.6570 | 0.8981 | 0.9953 | 0.8685 | 0.7872 | 0.8831 |
| B | FedAvg | 0.5034 | 52.5426 | 0.8354 | 0.7513 | 0.0840 | 0.0827 | 0.1527 |
| | FedProx | 0.8879 | 15.7715 | 0.8247 | 0.9929 | 0.7207 | 0.6001 | 0.7692 |
| | HarmoFL | 0.9390 | 7.5250 | 0.9570 | 0.9935 | 0.7534 | 0.7162 | 0.8431 |
| | MetaFed | 0.8995 | 8.4520 | 0.8583 | 0.9948 | 0.7854 | 0.6682 | 0.8202 |
| | MedSAM | 0.8810 | 4.8425 | 0.6994 | 0.9993 | 0.9614 | 0.6651 | 0.8098 |
| | VFMGL | 0.9328 | 5.0626 | 0.9337 | 0.9956 | 0.8196 | 0.7659 | 0.8729 |
| C | FedAvg | 0.7868 | 25.7947 | 0.9805 | 0.9543 | 0.4144 | 0.4060 | 0.5826 |
| | FedProx | 0.9037 | 6.6428 | 0.8132 | 0.9968 | 0.8836 | 0.7172 | 0.8469 |
| | HarmoFL | 0.9525 | 4.5665 | 0.9597 | 0.9939 | 0.8232 | 0.7895 | 0.8862 |
| | MetaFed | 0.8913 | 9.2436 | 0.8297 | 0.9912 | 0.7496 | 0.6494 | 0.7876 |
| | MedSAM | 0.8965 | 5.7118 | 0.7270 | 0.9988 | 0.9594 | 0.6929 | 0.8272 |
| | VFMGL | 0.9620 | 2.8192 | 0.9539 | 0.9973 | 0.9076 | 0.8672 | 0.9302 |
| D | FedAvg | 0.6957 | 45.0055 | 0.7222 | 0.9320 | 0.2818 | 0.2584 | 0.4054 |
| | FedProx | 0.8536 | 18.7689 | 0.7450 | 0.9919 | 0.7242 | 0.5928 | 0.7345 |
| | HarmoFL | 0.9084 | 13.8240 | 0.9455 | 0.9892 | 0.7334 | 0.6855 | 0.8261 |
| | MetaFed | 0.8716 | 15.8724 | 0.7776 | 0.9880 | 0.6874 | 0.5869 | 0.7297 |
| | MedSAM | 0.9098 | 4.2473 | 0.7565 | 0.9995 | 0.9840 | 0.7416 | 0.8554 |
| | VFMGL | 0.9191 | 9.4369 | 0.8434 | 0.9966 | 0.8370 | 0.7465 | 0.8402 |
| E | FedAvg | 0.7557 | 44.8552 | 0.8460 | 0.9364 | 0.3739 | 0.3555 | 0.5186 |
| | FedProx | 0.9018 | 14.1736 | 0.8811 | 0.9896 | 0.7645 | 0.6925 | 0.8187 |
| | HarmoFL | 0.9345 | 6.8490 | 0.8794 | 0.9948 | 0.8569 | 0.7654 | 0.8680 |
| | MetaFed | 0.8151 | 19.1216 | 0.6407 | 0.9884 | 0.7034 | 0.5449 | 0.6706 |
| | MedSAM | 0.9129 | 4.9324 | 0.7698 | 0.9985 | 0.9661 | 0.7403 | 0.8569 |
| | VFMGL | 0.9383 | 6.0202 | 0.9296 | 0.9946 | 0.8501 | 0.8028 | 0.8881 |
| F | FedAvg | 0.5078 | 53.7082 | 0.7025 | 0.7794 | 0.0880 | 0.0856 | 0.1564 |
| | FedProx | 0.7754 | 27.9849 | 0.7216 | 0.9880 | 0.6303 | 0.5371 | 0.6729 |
| | HarmoFL | 0.9167 | 12.9202 | 0.8876 | 0.9897 | 0.7471 | 0.7012 | 0.8113 |
| | MetaFed | 0.8268 | 18.1592 | 0.6701 | 0.9874 | 0.6345 | 0.5282 | 0.6518 |
| | MedSAM | 0.9076 | 4.3989 | 0.7476 | 0.9994 | 0.9644 | 0.7154 | 0.8423 |
| | VFMGL | 0.9080 | 6.8139 | 0.8981 | 0.9942 | 0.7973 | 0.7445 | 0.8447 |

Notes: VFMGL, Vision Foundation Model General Lightweight; ASSD, Average Symmetric Surface Distance; PPV, Positive Predictive Value; IOU: Intersection Over Union. Source data are provided as a Source Data file.

**Supplementary Table 4. Comparison of the performance of six methods in use case 4**

| Center | Methods | Dice | ASSD | Sensitivity | Specificity | PPV | IOU | F1 |
|---|---|---|---|---|---|---|---|---|
| A | FedAvg | 0.4493 | 5.5991 | 0.3041 | 0.5673 | 0.2572 | 0.1620 | 0.2787 |
| | FedProx | 0.7175 | 4.0955 | 0.6210 | 0.9322 | 0.7564 | 0.4858 | 0.6820 |
| | HarmoFL | 0.7126 | 4.1270 | 0.5655 | 0.9516 | 0.7929 | 0.4597 | 0.6602 |
| | MetaFed | 0.7066 | 4.2787 | 0.5823 | 0.9420 | 0.7715 | 0.4641 | 0.6637 |
| | MedSAM | 0.7703 | 1.8837 | 0.6338 | 0.8752 | 0.7653 | 0.5256 | 0.6934 |
| | VFMGL | 0.7509 | 3.6429 | 0.5774 | 0.9606 | 0.8257 | 0.4918 | 0.6796 |
| B | FedAvg | 0.4740 | 5.3538 | 0.3170 | 0.6262 | 0.2570 | 0.1647 | 0.2839 |
| | FedProx | 0.7140 | 4.3436 | 0.6542 | 0.9075 | 0.6687 | 0.4589 | 0.6614 |
| | HarmoFL | 0.7165 | 4.3308 | 0.5974 | 0.9358 | 0.7194 | 0.4509 | 0.6527 |
| | MetaFed | 0.6894 | 4.4940 | 0.6227 | 0.9056 | 0.6627 | 0.4413 | 0.6421 |
| | MedSAM | 0.7666 | 2.4434 | 0.6379 | 0.8743 | 0.6937 | 0.5073 | 0.6646 |
| | VFMGL | 0.7658 | 4.1422 | 0.6245 | 0.9347 | 0.7240 | 0.4731 | 0.6706 |
| C | FedAvg | 0.4336 | 10.2695 | 0.2468 | 0.5464 | 0.1723 | 0.1117 | 0.2029 |
| | FedProx | 0.7643 | 8.6537 | 0.7056 | 0.9073 | 0.6443 | 0.4772 | 0.6736 |
| | HarmoFL | 0.7696 | 8.4898 | 0.6516 | 0.9345 | 0.6886 | 0.4711 | 0.6696 |
| | MetaFed | 0.7199 | 8.7500 | 0.6851 | 0.8927 | 0.6213 | 0.4703 | 0.6516 |
| | MedSAM | 0.8219 | 2.5373 | 0.6901 | 0.9297 | 0.7839 | 0.5936 | 0.7340 |
| | VFMGL | 0.7735 | 8.2582 | 0.6203 | 0.9646 | 0.7653 | 0.4823 | 0.6852 |
| D | FedAvg | 0.4663 | 5.8823 | 0.3054 | 0.5668 | 0.2514 | 0.1587 | 0.2758 |
| | FedProx | 0.7080 | 4.3680 | 0.5639 | 0.9435 | 0.7748 | 0.4704 | 0.6527 |
| | HarmoFL | 0.6983 | 4.2005 | 0.5113 | 0.9616 | 0.8142 | 0.4459 | 0.6281 |
| | MetaFed | 0.6723 | 4.5729 | 0.5402 | 0.9410 | 0.7670 | 0.4466 | 0.6339 |
| | MedSAM | 0.7911 | 2.1497 | 0.6590 | 0.9024 | 0.7635 | 0.5534 | 0.7074 |
| | VFMGL | 0.7410 | 3.6780 | 0.5059 | 0.9681 | 0.8440 | 0.4471 | 0.6326 |
| E | FedAvg | 0.5288 | 1.0811 | 0.3998 | 0.6715 | 0.3341 | 0.2216 | 0.3640 |
| | FedProx | 0.6645 | 1.2186 | 0.5603 | 0.8924 | 0.6787 | 0.4406 | 0.6138 |
| | HarmoFL | 0.6901 | 1.1861 | 0.5380 | 0.9349 | 0.7690 | 0.4616 | 0.6331 |
| | MetaFed | 0.7016 | 1.1509 | 0.5698 | 0.9178 | 0.7382 | 0.4713 | 0.6432 |
| | MedSAM | 0.6591 | 1.2267 | 0.5590 | 0.7690 | 0.5127 | 0.3648 | 0.5349 |
| | VFMGL | 0.7568 | 1.0707 | 0.6386 | 0.8806 | 0.6821 | 0.4914 | 0.6596 |
| F | FedAvg | 0.4406 | 10.1532 | 0.3125 | 0.5589 | 0.1315 | 0.1010 | 0.1851 |
| | FedProx | 0.6677 | 7.3864 | 0.6236 | 0.8654 | 0.4064 | 0.2877 | 0.4921 |
| | HarmoFL | 0.6961 | 6.8815 | 0.6171 | 0.9039 | 0.4793 | 0.3260 | 0.5395 |
| | MetaFed | 0.6834 | 6.9784 | 0.6559 | 0.8965 | 0.4763 | 0.3391 | 0.5519 |
| | MedSAM | 0.8157 | 1.2948 | 0.6114 | 0.9693 | 0.7693 | 0.5180 | 0.6813 |
| | VFMGL | 0.7899 | 4.1967 | 0.6218 | 0.9729 | 0.7339 | 0.4772 | 0.6732 |

Notes: VFMGL, Vision Foundation Model General Lightweight; ASSD, Average Symmetric Surface Distance; PPV, Positive Predictive Value; IOU: Intersection Over Union. Source data are provided as a Source Data file.

**Supplementary Table 5.** Distribution of the use case 1 Test-Set data based on age grouping

| | Group | Center A | | Center B | | Center C | | Center D | |
|---|---|---|---|---|---|---|---|---|---|
| | | NMI | MI | NMI | MI | NMI | MI | NMI | MI |
| Test-Set | Group1(Age<=54.7) | 29 | 122 | 5 | 10 | 1 | 4 | 8 | 55 |
| | Group2(Age>54.7) | 5 | 119 | 1 | 13 | 0 | 10 | 0 | 55 |

Notes: MI, Myometrial Invasion; NMI, Non Myometrial Invasion.

**Supplementary Table 6. Multiple permutation distribution for use case 1**

| Distribution | Random Seed | partition ratio | Set | Center A | | Center B | | Center C | | Center D | |
|---|---|---|---|---|---|---|---|---|---|---|---|
| | | | | NMI | MI | NMI | MI | NMI | MI | NMI | MI |
| Initial | 42 | 0.60 | TrainSet | 49 | 361 | 8 | 34 | 1 | 21 | 11 | 165 |
| | | | TestSet | 34 | 241 | 6 | 23 | 1 | 14 | 8 | 110 |
| 1 | 50 | 0.50 | TrainSet | 41 | 301 | 7 | 28 | 1 | 17 | 9 | 137 |
| | | | TestSet | 42 | 301 | 7 | 29 | 1 | 18 | 10 | 138 |
| 2 | 100 | 0.55 | TrainSet | 45 | 331 | 7 | 31 | 1 | 19 | 10 | 151 |
| | | | TestSet | 38 | 271 | 7 | 26 | 1 | 16 | 9 | 124 |
| 3 | 200 | 0.65 | TrainSet | 53 | 391 | 9 | 37 | 1 | 22 | 12 | 178 |
| | | | TestSet | 30 | 211 | 5 | 20 | 1 | 13 | 7 | 97 |
| 4 | 500 | 0.70 | TrainSet | 58 | 421 | 9 | 39 | 1 | 24 | 13 | 192 |
| | | | TestSet | 25 | 181 | 5 | 18 | 1 | 11 | 6 | 83 |
| 5 | 1000 | 0.80 | TrainSet | 66 | 481 | 11 | 45 | 1 | 28 | 15 | 220 |
| | | | TestSet | 17 | 121 | 3 | 12 | 1 | 7 | 4 | 55 |

Notes: MI, Myometrial Invasion; NMI, Non Myometrial Invasion.

**Supplementary Table 7. Robustness critical layers for local model of each medical center in use case 1**

| Center | layer0 | | layer1 | | layer2 | | layer3 | | layer4 | |
|---|---|---|---|---|---|---|---|---|---|---|
| A | 0.87267068 | | 1.68551706 | √ | 1.66083648 | √ | 1.49487238 | √ | 1.18845993 | |
| B | 0.44240588 | | 2.43922249 | √ | 0.66256395 | √ | 1.36607569 | √ | 0.61106268 | |
| C | 1.77630597 | √ | 1.81546049 | √ | 0.89839248 | | 0.69220563 | | 1.06292467 | √ |
| D | 0.87161931 | √ | 1.28099127 | √ | 0.83994865 | √ | 0.79902224 | | 0.67803999 | |

In use case 1, we employ the DINOv2 model as the source model and ResNet18 as the expert model for clinical diagnosis, transferring the first convolutional layer and the subsequent four blocks of ResNet18 as the destination. The models layers marked in the table are identified as critical for robustness.

**Supplementary Table 8. Data distribution of use case 1-4**

EC-MI Classification(use case 1)

| | A | B | C | D | external center E | external center F |
|---|---|---|---|---|---|---|
| Train Set | 410 | 42 | 22 | 176 | - | - |
| Test Set | 275 | 29 | 15 | 118 | 63 | 117 |

breast cancer histopathological image classification(use case2)

| | A | B | C | D | E |
|---|---|---|---|---|---|
| Train Set | 38039 | 22339 | 54435 | 83096 | 93902 |
| Val Set | 9509 | 5584 | 13608 | 20774 | 23475 |
| Test Set | 11888 | 6981 | 17011 | 25968 | 29345 |

prostate MRI segmentation(use case 3)

| | A | B | C | D | E | F |
|---|---|---|---|---|---|---|
| Train Set | 167 | 100 | 299 | 263 | 245 | 112 |
| Val Set | 41 | 25 | 75 | 65 | 62 | 28 |
| Test Set | 53 | 32 | 94 | 83 | 77 | 35 |

histological cell nucleus segmentation(use case 4)

| | A | B | C | D | E | F |
|---|---|---|---|---|---|---|
| Train Set | 47 | 31 | 44 | 46 | 24 | 26 |
| Val Set | 11 | 8 | 11 | 11 | 6 | 7 |
| Test Set | 22 | 22 | 31 | 26 | 14 | 17 |

Notes: EC, Endometrial Cancer; MI, Myometrial Invasion. MRI, Magnetic Resonance Imaging.
Source data are provided as a Source Data file.

**Supplementary Table 9. Multiple permutation distribution for use case 2**

| Distribution | Random Seed | partition ratio | Set | Center A | Center B | Center C | Center D | Center E |
|---|---|---|---|---|---|---|---|---|
| initial | | | Train Set | 38039 | 22339 | 54435 | 83096 | 93902 |
| | | | Val Set | 9509 | 5584 | 13608 | 20774 | 23475 |
| | | | Test Set | 11888 | 6981 | 17011 | 25968 | 29345 |
| 1 | 50 | 0.50 | Train Set | 23775 | 13962 | 34023 | 51936 | 58690 |
| | | | Val Set | 5943 | 3490 | 8505 | 12984 | 14672 |
| | | | Test Set | 29718 | 17452 | 42526 | 64918 | 73360 |
| 2 | 100 | 0.55 | Train Set | 26152 | 15359 | 37424 | 57130 | 64559 |
| | | | Val Set | 6538 | 3839 | 9356 | 14282 | 16139 |
| | | | Test Set | 26746 | 15706 | 38274 | 58426 | 66024 |
| 3 | 200 | 0.65 | Train Set | 30908 | 18151 | 44229 | 67517 | 76296 |
| | | | Val Set | 7726 | 4537 | 11057 | 16879 | 19074 |
| | | | Test Set | 20802 | 12216 | 29768 | 45442 | 51352 |
| 4 | 500 | 0.70 | Train Set | 33285 | 19548 | 47631 | 72711 | 82165 |
| | | | Val Set | 8321 | 4886 | 11907 | 18177 | 20541 |
| | | | Test Set | 17830 | 10470 | 25516 | 38950 | 44016 |
| 5 | 1000 | 0.80 | Train Set | 38040 | 22340 | 54436 | 83098 | 93903 |
| | | | Val Set | 9510 | 5584 | 13608 | 20774 | 23475 |
| | | | Test Set | 11886 | 6980 | 17010 | 25966 | 29344 |

We shuffled the dataset using a random seed and then split it into training and test sets according to the specified ratio. Then, 20% of the training set was extracted to be used as the validation set. Source data are provided as a Source Data file.

**Supplementary Table 10. Multiple permutation distribution for use case 3**

| Distribution | Random Seed | partition ratio | Set | Center A | Center B | Center C | Center D | Center E | Center F |
|---|---|---|---|---|---|---|---|---|---|
| | initial | | Train Set | 167 | 100 | 299 | 263 | 245 | 112 |
| | | | Val Set | 41 | 25 | 75 | 65 | 62 | 28 |
| | | | Test Set | 53 | 32 | 94 | 83 | 77 | 35 |
| 1 | 50 | 0.50 | Train Set | 104 | 62 | 187 | 164 | 153 | 70 |
| | | | Val Set | 26 | 16 | 47 | 41 | 39 | 17 |
| | | | Test Set | 131 | 79 | 234 | 206 | 192 | 88 |
| 2 | 100 | 0.55 | Train Set | 114 | 69 | 205 | 180 | 168 | 77 |
| | | | Val Set | 29 | 17 | 52 | 46 | 43 | 19 |
| | | | Test Set | 118 | 71 | 211 | 185 | 173 | 79 |
| 3 | 200 | 0.65 | Train Set | 135 | 81 | 243 | 213 | 199 | 91 |
| | | | Val Set | 34 | 21 | 61 | 54 | 50 | 22 |
| | | | Test Set | 92 | 55 | 164 | 144 | 135 | 62 |
| 4 | 500 | 0.70 | Train Set | 146 | 87 | 262 | 230 | 215 | 98 |
| | | | Val Set | 36 | 22 | 65 | 57 | 53 | 24 |
| | | | Test Set | 79 | 48 | 141 | 124 | 116 | 53 |
| 5 | 1000 | 0.80 | Train Set | 167 | 100 | 299 | 263 | 245 | 112 |
| | | | Val Set | 41 | 25 | 75 | 65 | 62 | 28 |
| | | | Test Set | 53 | 32 | 94 | 83 | 77 | 35 |

We shuffled the dataset using a random seed and then split it into training and test sets according to the specified ratio. Then, 20% of the training set was extracted to be used as the validation set. Source data are provided as a Source Data file.

**Supplementary Table 11. Multiple permutation distribution for use case 4**

| Distribution | Random Seed | partition ratio | Set | Center | | | | | |
|---|---|---|---|---|---|---|---|---|---|
| | | | | A | B | C | D | E | F |
| | | | Train Set | 47 | 31 | 44 | 46 | 24 | 26 |
| | initial | | Val Set | 11 | 8 | 11 | 11 | 6 | 7 |
| | | | Test Set | 22 | 22 | 31 | 26 | 14 | 17 |
| | | | Train Set | 32 | 24 | 34 | 32 | 17 | 20 |
| 1 | 50 | 0.50 | Val Set | 8 | 6 | 9 | 9 | 5 | 5 |
| | | | Test Set | 40 | 31 | 43 | 42 | 22 | 25 |
| | | | Train Set | 35 | 26 | 37 | 36 | 19 | 21 |
| 2 | 100 | 0.55 | Val Set | 9 | 7 | 10 | 9 | 5 | 6 |
| | | | Test Set | 36 | 28 | 39 | 38 | 20 | 23 |
| | | | Train Set | 41 | 31 | 44 | 42 | 22 | 25 |
| 3 | 200 | 0.65 | Val Set | 11 | 8 | 11 | 11 | 6 | 7 |
| | | | Test Set | 28 | 22 | 31 | 30 | 16 | 18 |
| | | | Train Set | 44 | 33 | 48 | 46 | 24 | 28 |
| 4 | 500 | 0.70 | Val Set | 12 | 9 | 12 | 12 | 6 | 7 |
| | | | Test Set | 24 | 19 | 26 | 25 | 14 | 15 |
| | | | Train Set | 51 | 38 | 54 | 52 | 28 | 32 |
| 5 | 1000 | 0.80 | Val Set | 13 | 10 | 14 | 14 | 7 | 8 |
| | | | Test Set | 16 | 13 | 18 | 17 | 9 | 10 |

We shuffled the dataset using a random seed and then split it into training and test sets according to the specified ratio. Then, 20% of the training set was extracted to be used as the validation set. Source data are provided as a Source Data file.

**Supplementary Table 12. Performance of VFMGL under various data distributions in use case 2**

| Center | Methods | AUC | Sensitivity | Specificity | Accuracy | PPV | NPV | F1 |
|---|---|---|---|---|---|---|---|---|
| A | initial | 0.9992 | 0.9882 (5874/5944) | 0.9896 (5882/5944) | 0.9889 (11756/11888) | 0.9896 (5874/5936) | 0.9882 (5882/5952) | 0.9889 |
| | 1 | 0.9989 | 0.9896 (14704/14859) | 0.9860 (14651/14859) | 0.9878 (29355/29718) | 0.9861 (14704/14912) | 0.9895 (14651/14806) | 0.9878 |
| | 2 | 0.9988 | 0.9765 (13059/13373) | 0.9951 (13308/13373) | 0.9858 (26367/26746) | 0.9950 (13059/13124) | 0.9769 (13308/13622) | 0.9857 |
| | 3 | 0.9991 | 0.9863 (10259/10401) | 0.9894 (10291/10401) | 0.9879 (20550/20802) | 0.9894 (10259/10369) | 0.9864 (10291/10433) | 0.9879 |
| | 4 | 0.9991 | 0.9874 (8803/8915) | 0.9920 (8844/8915) | 0.9897 (17647/17830) | 0.9920 (8803/8874) | 0.9875 (8844/8956) | 0.9897 |
| | 5 | 0.9990 | 0.9837 (5846/5943) | 0.9909 (5889/5943) | 0.9873 (11735/11886) | 0.9908 (5846/5900) | 0.9838 (5889/5986) | 0.9872 |
| B | initial | 0.9973 | 0.9481 (3309/3490) | 0.9974 (3482/3491) | 0.9728 (6791/6981) | 0.9973 (3309/3318) | 0.9506 (3482/3663) | 0.9721 |
| | 1 | 0.9977 | 0.9589 (8367/8726) | 0.9936 (8670/8726) | 0.9762 (17037/17452) | 0.9934 (8367/8423) | 0.9602 (8670/9029) | 0.9758 |
| | 2 | 0.9978 | 0.9826 (7716/7853) | 0.9808 (7702/7853) | 0.9817 (15418/15706) | 0.9808 (7716/7867) | 0.9825 (7702/7839) | 0.9817 |
| | 3 | 0.9980 | 0.9751 (5956/6108) | 0.9903 (6049/6108) | 0.9827 (12005/12216) | 0.9902 (5956/6015) | 0.9755 (6049/6201) | 0.9826 |
| | 4 | 0.9981 | 0.9866 (5165/5235) | 0.9811 (5136/5235) | 0.9839 (10301/10470) | 0.9812 (5165/5264) | 0.9866 (5136/5206) | 0.9839 |
| | 5 | 0.9977 | 0.9731 (3396/3490) | 0.9911 (3459/3490) | 0.9821 (6855/6980) | 0.9910 (3396/3427) | 0.9735 (3459/3553) | 0.9819 |
| C | initial | 0.9995 | 0.9911 (8430/8506) | 0.9915 (8433/8505) | 0.9913 (16863/17011) | 0.9915 (8430/8502) | 0.9911 (8433/8509) | 0.9913 |
| | 1 | 0.9985 | 0.9856 (20956/21263) | 0.9843 (20929/21263) | 0.9849 (41885/42526) | 0.9843 (20956/21290) | 0.9855 (20929/21236) | 0.9849 |
| | 2 | 0.9989 | 0.9718 (18598/19137) | 0.9948 (19037/19137) | 0.9833 (37635/38274) | 0.9947 (18598/18698) | 0.9725 (19037/19576) | 0.9831 |
| | 3 | 0.9989 | 0.9765 (14534/14884) | 0.9942 (14797/14884) | 0.9853 (29331/29768) | 0.9940 (14534/14621) | 0.9769 (14797/15147) | 0.9852 |
| | 4 | 0.9985 | 0.9911 (12644/12758) | 0.9676 (12345/12758) | 0.9793 (24989/25516) | 0.9684 (12644/13057) | 0.9908 (12345/12459) | 0.9796 |
| | 5 | 0.9987 | 0.9780 (8318/8505) | 0.9937 (8451/8505) | 0.9858 (16769/17010) | 0.9935 (8318/8372) | 0.9784 (8451/8638) | 0.9857 |
| D | initial | 0.9977 | 0.9427 (12240/12984) | 0.9988 (12969/12984) | 0.9708 (25209/25968) | 0.9988 (12240/12255) | 0.9457 (12969/13713) | 0.9699 |
| | 1 | 0.9957 | 0.9607 (31183/32459) | 0.9819 (31870/32459) | 0.9713 (63053/64918) | 0.9815 (31183/31772) | 0.9615 (31870/33146) | 0.9710 |
| | 2 | 0.9968 | 0.9516 (27800/29213) | 0.9940 (29039/29213) | 0.9728 (56839/58426) | 0.9938 (27800/27974) | 0.9536 (29039/30452) | 0.9722 |
| | 3 | 0.9970 | 0.9682 (21999/22721) | 0.9883 (22456/22721) | 0.9783 (44455/45442) | 0.9881 (21999/22264) | 0.9688 (22456/23178) | 0.9781 |
| | 4 | 0.9956 | 0.9625 (18744/19475) | 0.9820 (19124/19475) | 0.9722 (37868/38950) | 0.9816 (18744/19095) | 0.9632 (19124/19855) | 0.9719 |
| | 5 | 0.9967 | 0.9670 (12554/12983) | 0.9879 (12826/12983) | 0.9774 (25380/25966) | 0.9876 (12554/12711) | 0.9676 (12826/13255) | 0.9772 |
| E | initial | 0.9993 | 0.9845 (14445/14672) | 0.9922 (14559/14673) | 0.9884 (29004/29345) | 0.9922 (14445/14559) | 0.9846 (14559/14786) | 0.9883 |
| | 1 | 0.9986 | 0.9853 (36141/36680) | 0.9849 (36126/36680) | 0.9851 (72267/73360) | 0.9849 (36141/36695) | 0.9853 (36126/36665) | 0.9851 |
| | 2 | 0.9987 | 0.9915 (32730/33012) | 0.9798 (32345/33012) | 0.9856 (65075/66024) | 0.9800 (32730/33397) | 0.9914 (32345/32627) | 0.9857 |
| | 3 | 0.9989 | 0.9837 (25257/25676) | 0.9921 (25472/25676) | 0.9879 (50729/51352) | 0.9920 (25257/25461) | 0.9838 (25472/25891) | 0.9878 |
| | 4 | 0.9989 | 0.9913 (21816/22008) | 0.9852 (21683/22008) | 0.9883 (43499/44016) | 0.9853 (21816/22141) | 0.9912 (21683/21875) | 0.9883 |
| | 5 | 0.9990 | 0.9913 (14544/14672) | 0.9851 (14453/14672) | 0.9882 (28997/29344) | 0.9852 (14544/14763) | 0.9912 (14453/14581) | 0.9882 |

Notes: AUC, Area Under the Curve; PPV, Positive Predictive Value; NPV, Negative Predictive Value. Source data are provided as a Source Data file.

**Supplementary Table 13. Performance of VFMGL under various data distributions in use case 3**

| Center | Methods | Dice | ASSD | Sensitivity | Specificity | PPV | IOU | F1 |
|---|---|---|---|---|---|---|---|---|
| A | initial | 0.9340 | 5.6570 | 0.8981 | 0.9953 | 0.8685 | 0.7872 | 0.8831 |
| | 1 | 0.9005 | 8.5498 | 0.9074 | 0.9892 | 0.7638 | 0.7060 | 0.8294 |
| | 2 | 0.9040 | 9.7341 | 0.9079 | 0.9905 | 0.7904 | 0.7240 | 0.8451 |
| | 3 | 0.9196 | 8.0357 | 0.8951 | 0.9926 | 0.8180 | 0.7420 | 0.8548 |
| | 4 | 0.9136 | 7.8488 | 0.9155 | 0.9909 | 0.7823 | 0.7214 | 0.8437 |
| | 5 | 0.9089 | 10.0914 | 0.9047 | 0.9921 | 0.7736 | 0.7083 | 0.8340 |
| B | initial | 0.9328 | 5.0626 | 0.9337 | 0.9956 | 0.8196 | 0.7659 | 0.8729 |
| | 1 | 0.9115 | 6.8731 | 0.9129 | 0.9950 | 0.7937 | 0.7339 | 0.8492 |
| | 2 | 0.9258 | 4.8663 | 0.9196 | 0.9960 | 0.8194 | 0.7525 | 0.8666 |
| | 3 | 0.9304 | 5.5225 | 0.9043 | 0.9965 | 0.8305 | 0.7601 | 0.8658 |
| | 4 | 0.9170 | 4.9035 | 0.9139 | 0.9950 | 0.7983 | 0.7443 | 0.8522 |
| | 5 | 0.9371 | 3.4074 | 0.9290 | 0.9972 | 0.8418 | 0.7845 | 0.8832 |
| C | initial | 0.9620 | 2.8192 | 0.9539 | 0.9973 | 0.9076 | 0.8672 | 0.9302 |
| | 1 | 0.9485 | 3.8772 | 0.9271 | 0.9970 | 0.8897 | 0.8270 | 0.9080 |
| | 2 | 0.9569 | 3.5448 | 0.9298 | 0.9972 | 0.9013 | 0.8421 | 0.9153 |
| | 3 | 0.9543 | 3.5278 | 0.9291 | 0.9969 | 0.8956 | 0.8377 | 0.9120 |
| | 4 | 0.9466 | 4.6275 | 0.9424 | 0.9955 | 0.8563 | 0.8100 | 0.8973 |
| | 5 | 0.9592 | 2.5650 | 0.9381 | 0.9978 | 0.9246 | 0.8695 | 0.9313 |
| D | initial | 0.9191 | 9.4369 | 0.8434 | 0.9966 | 0.8370 | 0.7465 | 0.8402 |
| | 1 | 0.9281 | 7.4399 | 0.9150 | 0.9947 | 0.8320 | 0.7788 | 0.8715 |
| | 2 | 0.9255 | 7.2161 | 0.9125 | 0.9956 | 0.8327 | 0.7777 | 0.8708 |
| | 3 | 0.9334 | 6.8064 | 0.9198 | 0.9946 | 0.8150 | 0.7627 | 0.8642 |
| | 4 | 0.9476 | 6.0605 | 0.9210 | 0.9957 | 0.8426 | 0.7822 | 0.8800 |
| | 5 | 0.9243 | 9.7444 | 0.9096 | 0.9943 | 0.8044 | 0.7509 | 0.8538 |
| E | initial | 0.9383 | 6.0202 | 0.9296 | 0.9946 | 0.8501 | 0.8028 | 0.8881 |
| | 1 | 0.9131 | 9.6877 | 0.9203 | 0.9913 | 0.8024 | 0.7439 | 0.8573 |
| | 2 | 0.9308 | 6.9545 | 0.9291 | 0.9915 | 0.8188 | 0.7703 | 0.8705 |
| | 3 | 0.9166 | 9.4326 | 0.9038 | 0.9896 | 0.7892 | 0.7457 | 0.8426 |
| | 4 | 0.9159 | 8.4609 | 0.9331 | 0.9900 | 0.7800 | 0.7418 | 0.8497 |
| | 5 | 0.9329 | 5.1608 | 0.9026 | 0.9949 | 0.8570 | 0.7879 | 0.8792 |
| F | initial | 0.9080 | 6.8139 | 0.8981 | 0.9942 | 0.7973 | 0.7445 | 0.8447 |
| | 1 | 0.9022 | 6.5187 | 0.8782 | 0.9957 | 0.8097 | 0.7134 | 0.8425 |
| | 2 | 0.8932 | 7.9375 | 0.8689 | 0.9939 | 0.7801 | 0.7069 | 0.8221 |
| | 3 | 0.9083 | 8.1140 | 0.8775 | 0.9956 | 0.8148 | 0.7402 | 0.8450 |
| | 4 | 0.9041 | 7.3885 | 0.9216 | 0.9932 | 0.7722 | 0.7246 | 0.8403 |
| | 5 | 0.8918 | 7.7375 | 0.8909 | 0.9953 | 0.7952 | 0.7166 | 0.8403 |

Notes: ASSD, Average Symmetric Surface Distance; PPV, Positive Predictive Value; IOU, Intersection Over Union. Source data are provided as a Source Data file.

**Supplementary Table 14. Performance of VFMGL under various data distributions in use case 4**

| Center | Distribution | Dice | ASSD | Sensitivity | Specificity | PPV | IOU | F1 |
|---|---|---|---|---|---|---|---|---|
| A | Initial | 0.7509 | 3.6429 | 0.5774 | 0.9606 | 0.8257 | 0.4918 | 0.6796 |
| | 1 | 0.7574 | 6.6052 | 0.6516 | 0.9404 | 0.6632 | 0.4406 | 0.6573 |
| | 2 | 0.7955 | 6.4820 | 0.7688 | 0.9170 | 0.6340 | 0.5054 | 0.6949 |
| | 3 | 0.7820 | 6.1335 | 0.7001 | 0.9318 | 0.6701 | 0.4895 | 0.6848 |
| | 4 | 0.7715 | 6.1798 | 0.7149 | 0.9286 | 0.6423 | 0.4700 | 0.6766 |
| | 5 | 0.7415 | 6.7174 | 0.6362 | 0.9346 | 0.6238 | 0.4323 | 0.6300 |
| B | Initial | 0.7658 | 4.1422 | 0.6245 | 0.9347 | 0.7240 | 0.4731 | 0.6706 |
| | 1 | 0.7717 | 4.6163 | 0.6674 | 0.9366 | 0.6840 | 0.4777 | 0.6756 |
| | 2 | 0.7816 | 4.7190 | 0.6996 | 0.9156 | 0.6239 | 0.4653 | 0.6596 |
| | 3 | 0.7559 | 7.7385 | 0.7909 | 0.8771 | 0.5099 | 0.4388 | 0.6201 |
| | 4 | 0.7528 | 4.9399 | 0.6696 | 0.9221 | 0.6399 | 0.4586 | 0.6545 |
| | 5 | 0.7632 | 7.0551 | 0.7379 | 0.9100 | 0.5853 | 0.4341 | 0.6528 |
| C | Initial | 0.7735 | 8.2582 | 0.6203 | 0.9646 | 0.7653 | 0.4823 | 0.6852 |
| | 1 | 0.7700 | 9.7468 | 0.7477 | 0.9253 | 0.5885 | 0.4502 | 0.6586 |
| | 2 | 0.7703 | 10.6894 | 0.7357 | 0.9227 | 0.6009 | 0.4593 | 0.6615 |
| | 3 | 0.7733 | 10.9627 | 0.7115 | 0.9201 | 0.5707 | 0.4314 | 0.6334 |
| | 4 | 0.8176 | 5.8284 | 0.7548 | 0.9307 | 0.6793 | 0.5251 | 0.7151 |
| | 5 | 0.7893 | 9.0939 | 0.7107 | 0.9484 | 0.6529 | 0.4861 | 0.6806 |
| D | Initial | 0.7410 | 3.6780 | 0.5059 | 0.9681 | 0.8440 | 0.4471 | 0.6326 |
| | 1 | 0.7793 | 6.4168 | 0.7545 | 0.9068 | 0.6190 | 0.4808 | 0.6801 |
| | 2 | 0.7825 | 5.6679 | 0.7487 | 0.9064 | 0.6292 | 0.4945 | 0.6838 |
| | 3 | 0.7794 | 4.8177 | 0.6492 | 0.9390 | 0.7212 | 0.4926 | 0.6833 |
| | 4 | 0.7647 | 5.7593 | 0.6518 | 0.9286 | 0.6955 | 0.4647 | 0.6729 |
| | 5 | 0.7794 | 5.2083 | 0.6974 | 0.9207 | 0.6746 | 0.5014 | 0.6858 |
| E | Initial | 0.7568 | 1.0707 | 0.6386 | 0.8806 | 0.6821 | 0.4914 | 0.6596 |
| | 1 | 0.7552 | 1.1665 | 0.6574 | 0.8775 | 0.6549 | 0.4851 | 0.6562 |
| | 2 | 0.7506 | 1.1697 | 0.6480 | 0.8822 | 0.6840 | 0.4938 | 0.6655 |
| | 3 | 0.7746 | 1.0311 | 0.6804 | 0.8951 | 0.7071 | 0.5265 | 0.6935 |
| | 4 | 0.7492 | 1.0805 | 0.6696 | 0.8875 | 0.6733 | 0.4946 | 0.6714 |
| | 5 | 0.7509 | 1.2700 | 0.6420 | 0.8854 | 0.6368 | 0.4557 | 0.6394 |
| F | Initial | 0.7899 | 4.1967 | 0.6218 | 0.9729 | 0.7339 | 0.4772 | 0.6732 |
| | 1 | 0.8276 | 3.9756 | 0.7545 | 0.9645 | 0.7097 | 0.5415 | 0.7314 |
| | 2 | 0.8065 | 6.1754 | 0.8185 | 0.9563 | 0.6114 | 0.4968 | 0.7000 |
| | 3 | 0.8357 | 3.7802 | 0.7583 | 0.9692 | 0.7242 | 0.5574 | 0.7408 |
| | 4 | 0.8446 | 4.2443 | 0.7073 | 0.9753 | 0.7540 | 0.5446 | 0.7299 |
| | 5 | 0.8358 | 8.2434 | 0.7934 | 0.9725 | 0.6613 | 0.5383 | 0.7213 |

Notes: ASSD, Average Symmetric Surface Distance; PPV, Positive Predictive Value; IOU, Intersection Over Union. Source data are provided as a Source Data file.

**Supplementary Table 15. The matching differences of model layers between the local model of different centers and the vision foundation model**

| matching Center | (0, 0) | (0, 1) | (0, 2) | (0, 3) | (0, 4) | (1, 0) | (1, 1) | (1, 2) | (1, 3) | (1, 4) |
|---|---|---|---|---|---|---|---|---|---|---|
| Center A | 0.08 | 1.2 | 0.98 | 4.22 | 3.33 | 0.99 | 3.48 | 3.04 | 0.43 | 0.03 |
| Center B | 0.78 | 2.81 | 1.89 | 2.4 | 0.05 | 0. | 4.55 | 0.15 | 0.52 | 0.78 |
| Center C | 2.74 | 3.71 | 0. | 0. | 3.42 | 2.14 | 1.47 | 1.96 | 1.41 | 0. |
| Center D | 0. | 1.61 | 0.15 | 0.17 | 0. | 1.64 | 1.04 | 1.45 | 0.05 | 0.01 |

| matching Center | (2, 0) | (2, 1) | (2, 2) | (2, 3) | (2, 4) | (3, 0) | (3, 1) | (3, 2) | (3, 3) | (3, 4) |
|---|---|---|---|---|---|---|---|---|---|---|
| Center A | 1.47 | 0.41 | 0.62 | 1.22 | 1.02 | 0.95 | 1.65 | 2.01 | 0.1 | 0.38 |
| Center B | 0. | 2.18 | 0. | 1.91 | 0.76 | 0.99 | 0.22 | 0.61 | 0.63 | 0.85 |
| Center C | 2.21 | 0.81 | 0. | 0.94 | 0.4 | 0.01 | 1.27 | 1.63 | 0.42 | 0.43 |
| Center D | 0.47 | 1.65 | 1.56 | 1.81 | 1.81 | 1.37 | 0.82 | 0.2 | 1.16 | 0.9 |

The table shows that in use case 1, the matching degree between vision foundation model (VFM) model layers and local model layers varies across centers. For example, (0,0) indicates a pre-matching between layer 0 of the VFM and layer 0 of the local model, with the local model in Center C exhibiting a higher degree of adaptation. In the (0,3) matching, Centers A and B demonstrate a higher level of adaptation. Source data are provided as a Source Data file.

**Supplementary Table 16. Performance comparison between VFMGL and the KD method based on model logic layer output.**

| Center | Methods | AUC | Sensitivity | Specificity | Accuracy | PPV | NPV | F1 |
|---|---|---|---|---|---|---|---|---|
| A | VFMGL | 0.9992 | 0.9882 (5874/5944) | 0.9896 (5882/5944) | 0.9889 (11756/11888) | 0.9896 (5874/5936) | 0.9882 (5882/5952) | 0.9889 |
| | Virchow_KD | 0.9266 | 0.8612 (5119/5944) | 0.7873 (4680/5944) | 0.8243 (9799/11888) | 0.8020 (5119/6383) | 0.8501 (4680/5505) | 0.8305 |
| B | VFMGL | 0.9973 | 0.9481 (3309/3490) | 0.9974 (3482/3491) | 0.9728 (6791/6981) | 0.9973 (3309/3318) | 0.9506 (3482/3663) | 0.9721 |
| | Virchow_KD | 0.9981 | 0.9436 (3293/3490) | 0.9946 (3472/3491) | 0.9691 (6765/6981) | 0.9943 (3293/3312) | 0.9463 (3472/3669) | 0.9682 |
| C | VFMGL | 0.9995 | 0.9911 (8430/8506) | 0.9915 (8433/8505) | 0.9913 (16863/17011) | 0.9915 (8430/8502) | 0.9911 (8433/8509) | 0.9913 |
| | Virchow_KD | 0.6401 | 0.1743 (1483/8506) | 0.9949 (8462/8505) | 0.5846 (9945/17011) | 0.9718 (1483/1526) | 0.5465 (8462/15485) | 0.2957 |
| D | VFMGL | 0.9977 | 0.9427 (12240/12984) | 0.9988 (12969/12984) | 0.9708 (25209/25968) | 0.9988 (12240/12255) | 0.9457 (12969/13713) | 0.9699 |
| | Virchow_KD | 0.9748 | 0.7160 (9297/12984) | 0.9970 (12945/12984) | 0.8565 (22242/25968) | 0.9958 (9297/9336) | 0.7783 (12945/16632) | 0.8331 |
| E | VFMGL | 0.9993 | 0.9845 (14445/14672) | 0.9922 (14559/14673) | 0.9884 (29004/29345) | 0.9922 (14445/14559) | 0.9846 (14559/14786) | 0.9883 |
| | Virchow_KD | 0.9157 | 0.1322 (1940/14672) | 0.9957 (14610/14673) | 0.5640 (16550/29345) | 0.9685 (1940/2003) | 0.5343 (14610/27342) | 0.2327 |

Notes: VFMGL, Vision Foundation Model General Lightweight; KD, Knowledge Distillation; AUC, Area Under the Curve; PPV, Positive Predictive Value; NPV, Negative Predictive Value. Source data are provided as a Source Data file.

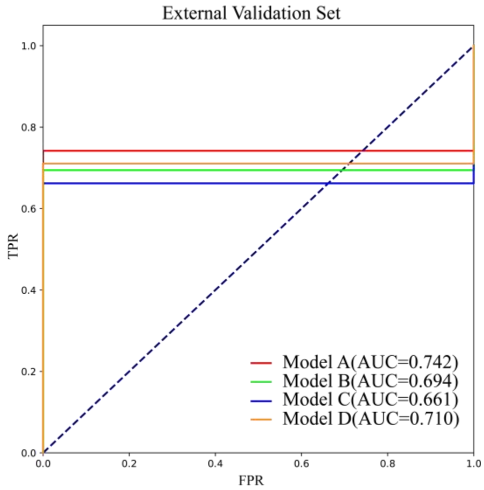


**Supplementary Fig.1 The ROC curves for VFMGL on external center E is shown.** Notes: ROC, Receiver Operating Characteristic curve; AUC, Area Under the Curve; TPR, True Positive Rate; FPR, False Positive Rate. Source data are provided as a Source Data file.

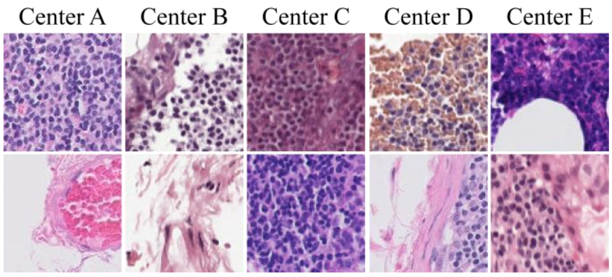


**Supplementary Fig.2 Examples of breast histology images of normal and tumor tissues from five centers.**

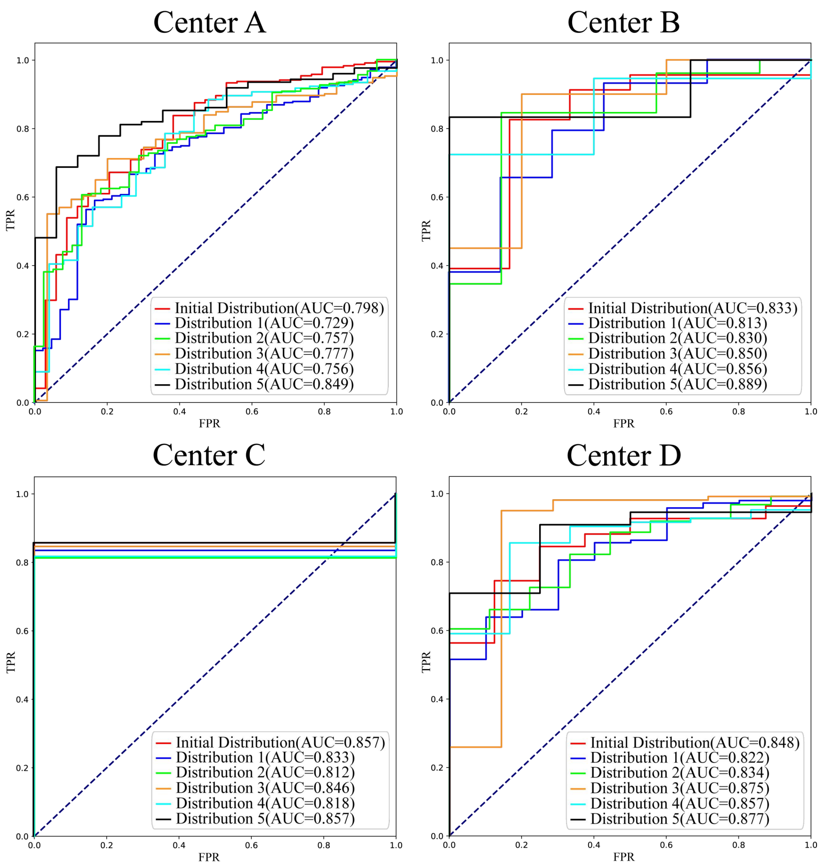


**Supplementary Fig.3 ROC curves of VFMGL under different data distributions at the four centers.** Notes: VFMGL, Vision Foundation Model General Lightweight; ROC, Receiver Operating Characteristic curve; AUC, Area Under the Curve; TPR, True Positive Rate; FPR, False Positive Rate. Source data are provided as a Source Data file.

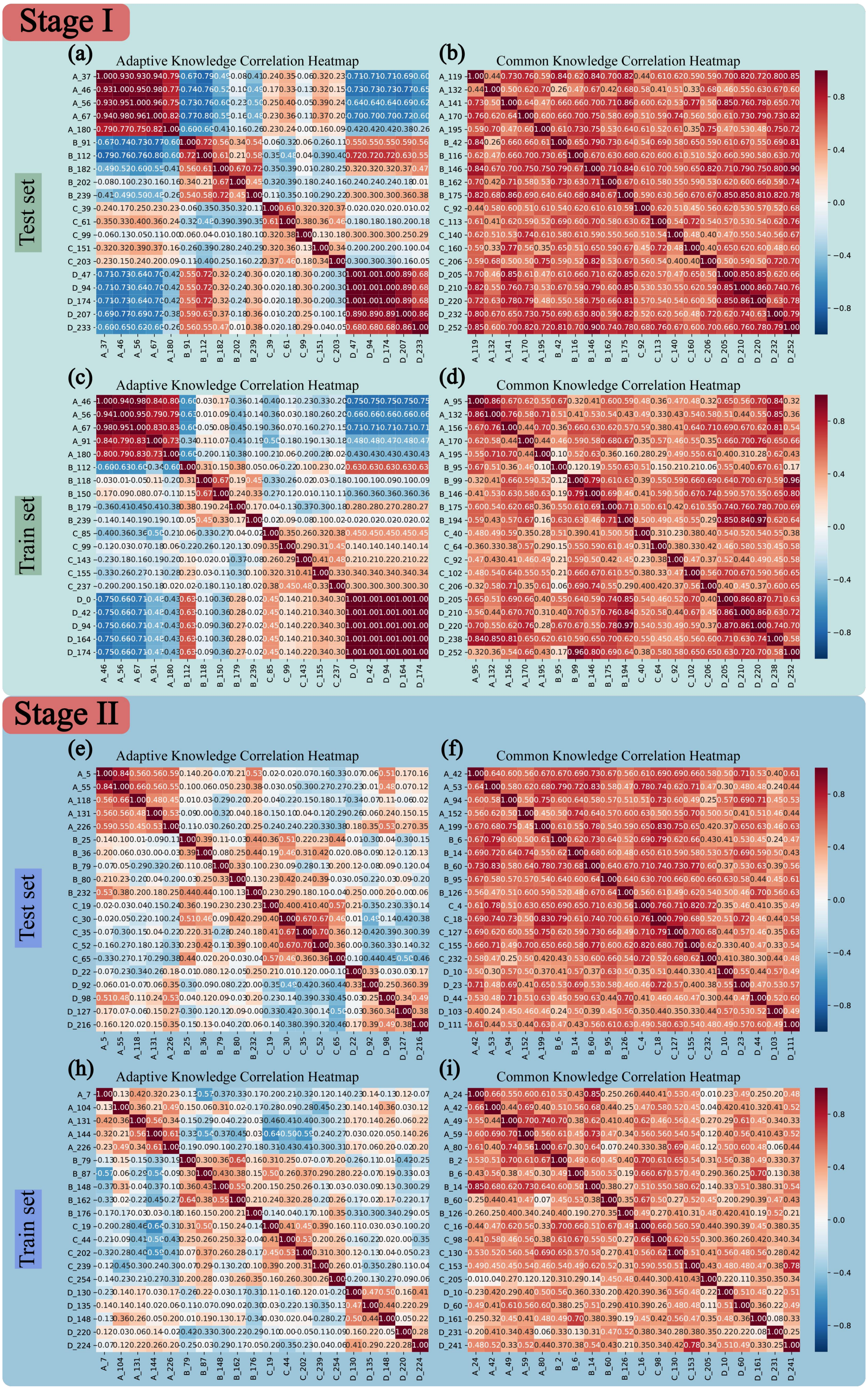


**Supplementary Fig.4 Correlation heatmaps of adaptive knowledge and common knowledge.** **(a)** Adaptive knowledge correlation heatmap of the first stage of VFMGL in the test set. **(b)** Common knowledge correlation heatmap of the first stage of VFMGL in the test set. **(c)** Adaptive knowledge correlation heatmap of the first stage of VFMGL in the training set. **(d)** Common knowledge correlation heatmap of the first stage of VFMGL in the training set. **(e)** Adaptive knowledge correlation heatmap of the second stage of VFMGL in the test set. **(f)** Common knowledge correlation heatmap of the second stage of VFMGL in the test set. **(g)** Adaptive knowledge correlation heatmap of the second stage of VFMGL in the training set. **(h)** Common knowledge correlation heatmap of the second stage of VFMGL in the training set. The first column shows the heatmap of correlation for adaptive features, while the second column displays the heatmap of correlation for common features. Notes: VFMGL, Vision Foundation Model General Lightweight. Source data are provided as a Source Data file.

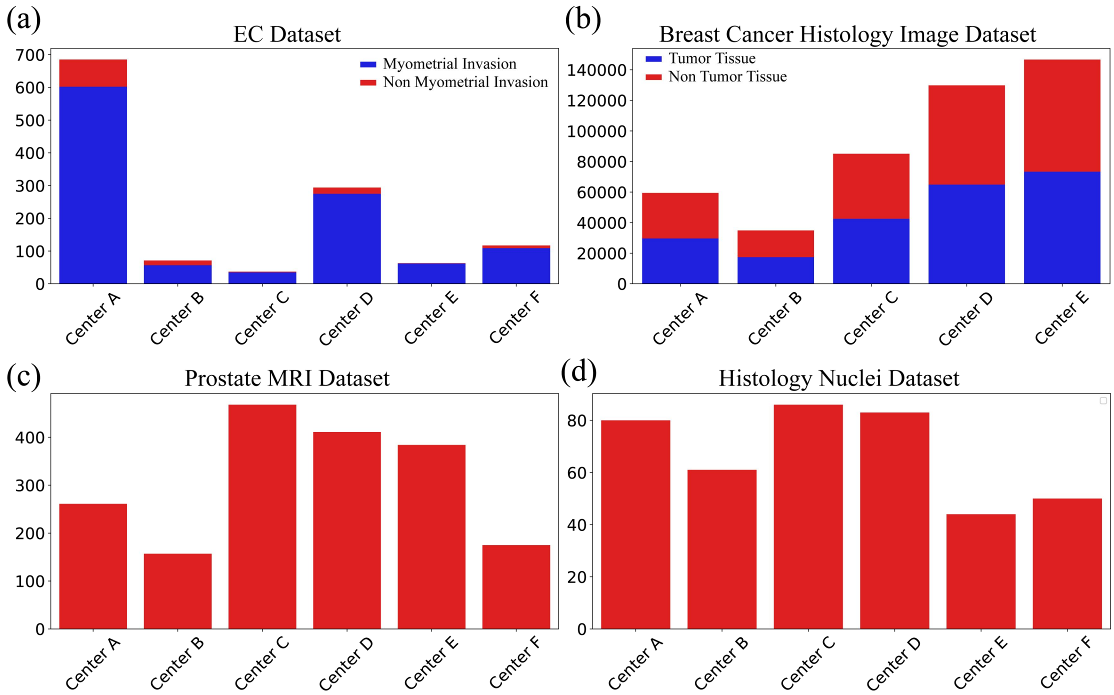


**Supplementary Fig.5 Data distributions of use case 1-4. (a)** The multi-center distributions for use cases 1. **(b)** The multi-center distributions for use cases 2. **(c)** The multi-center distributions for use cases 3. **(d)** The multi-center distributions for use cases 4. Source data are provided as a Source Data file.

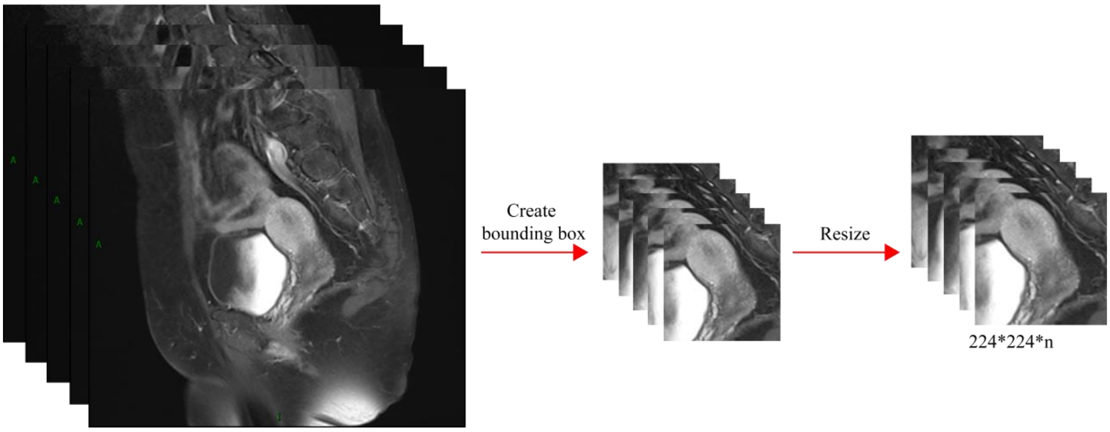


**Supplementary Fig.6 The preprocessing of CT images for a single patient is shown above.** Notes: n is the number of CT images the patient has; CT, Computed Tomography.

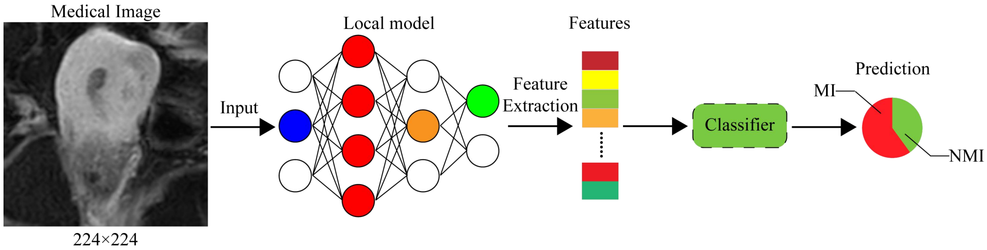


**Supplementary Fig.7 Feature extraction and patient classification.** Notes: MI, Myometrial Invasion; NMI, Non Myometrial Invasion.

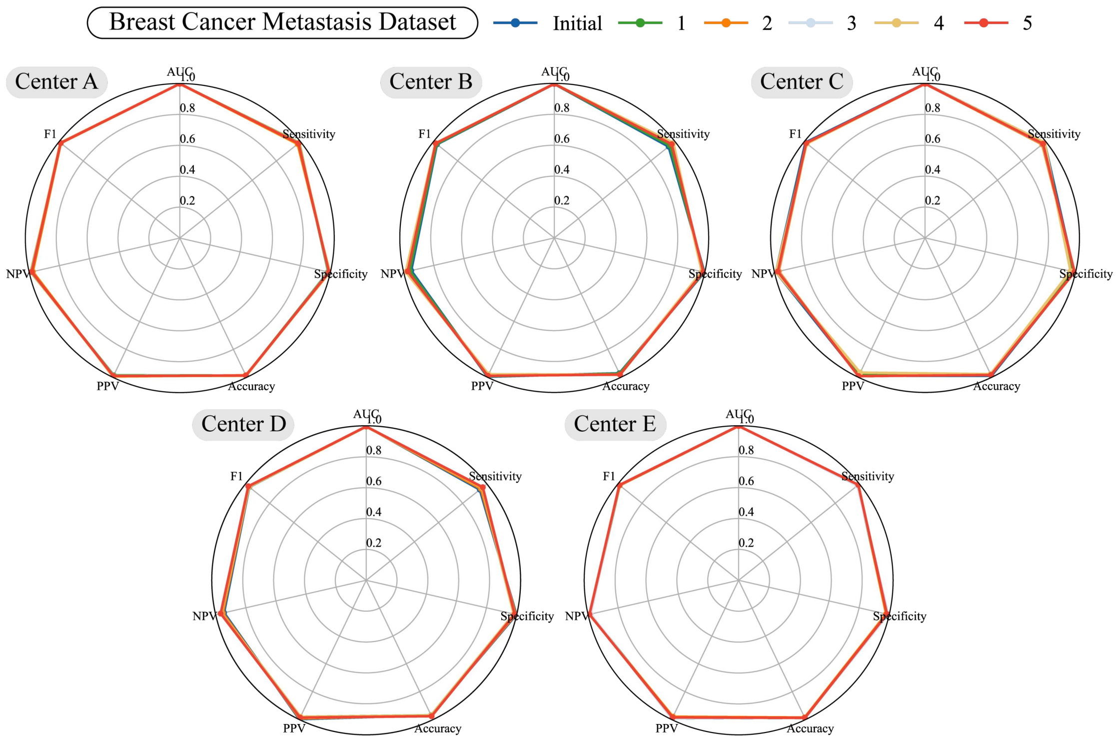


**Supplementary Fig.8 Radar chart comparison of VFMGL's performance under six different data distributions in the breast cancer histology image classification task(use case 2)**. Notes: AUC, Area Under the Curve; PPV, Positive Predictive Value; NPV, Negative Predictive Value; VFMGL, Vision Foundation Model General Lightweight. Source data are provided as a Source Data file.

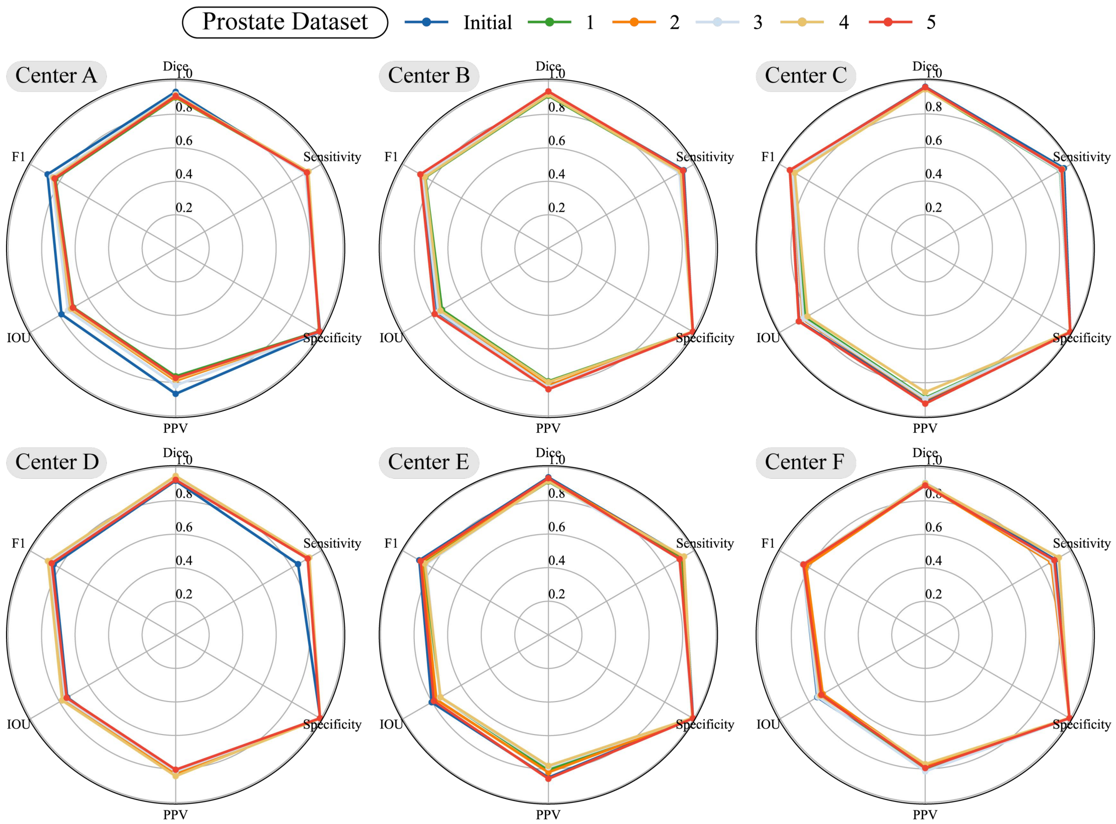


**Supplementary Fig.9 Radar chart comparison of VFMGL's performance under six different data distributions in the prostate MRI segmentation task(use case 3).** Notes: PPV, Positive Predictive Value; IOU, Intersection Over Union; VFMGL, Vision Foundation Model General Lightweight; MRI, Magnetic Resonance Imaging. Source data are provided as a Source Data file.

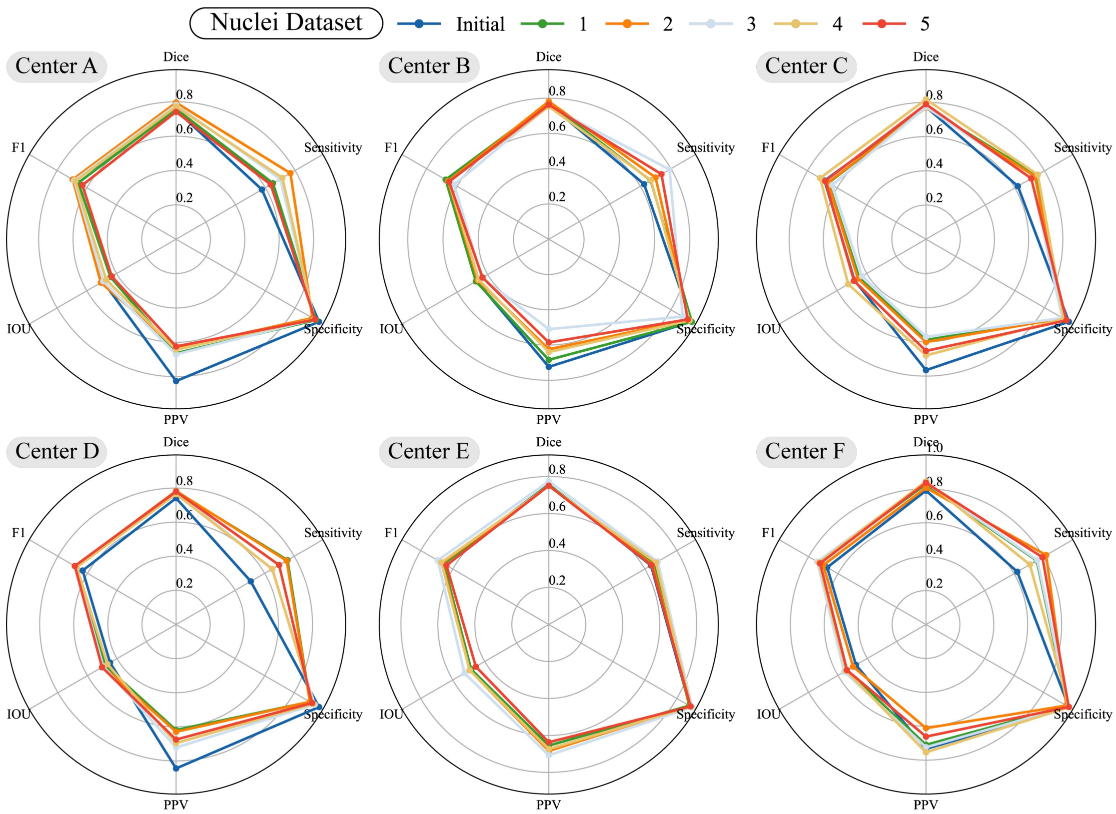


**Supplementary Fig.10 Radar chart comparison of VFMGL's performance under six different data distributions in the histology nuclei segmentation task(use case 4).** Notes: PPV, Positive Predictive Value; IOU: Intersection Over Union; VFMGL, Vision Foundation Model General Lightweight. Source data are provided as a Source Data file.

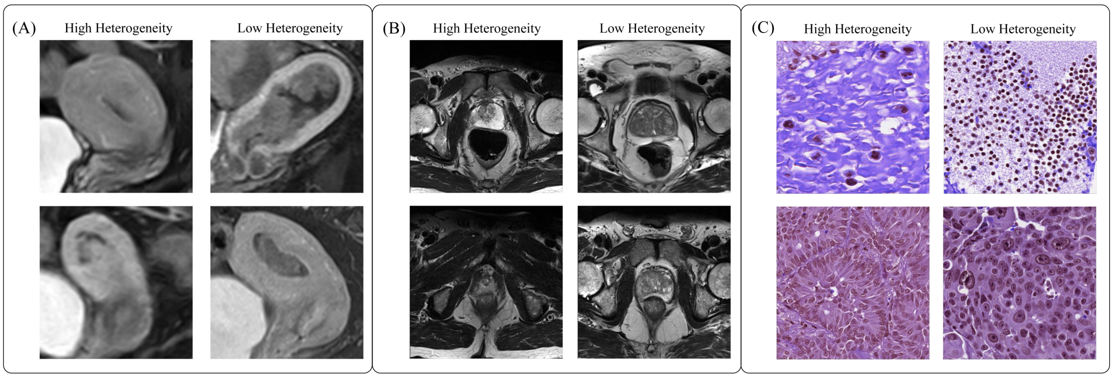


**Supplementary Fig.11 Examples of high heterogeneity and low heterogeneity. (A)** Display of high and low heterogeneity data in use case 1. **(B)** Display of high and low heterogeneity data in use case 3. **(C)** Display of high and low heterogeneity data in use case 4. As shown in Supplementary Fig.11(A), in the example provided for use case 1, the first column represents examples identified by DDBL as high-heterogeneity data, while the second column shows low-heterogeneity data; the first row contains positive samples, and the second row, negative samples. The figure demonstrates that low-heterogeneity data provide simpler and clearer information useful for diagnosis, with a lower risk of misjudgment. In contrast, high-heterogeneity data offer more complex information, which increases diagnostic difficulty and risk—such as how the intrauterine environment and the smoothness of the inner wall can impact diagnosis. In segmentation tasks (Supplementary Fig.11(B)(C)), the segmentation targets in low-heterogeneity images exhibit relatively clear and common boundary information, whereas high-heterogeneity images present segmentation targets with more challenging contours to define, for example, the impact of staining differences on the delineation of nuclear contours.

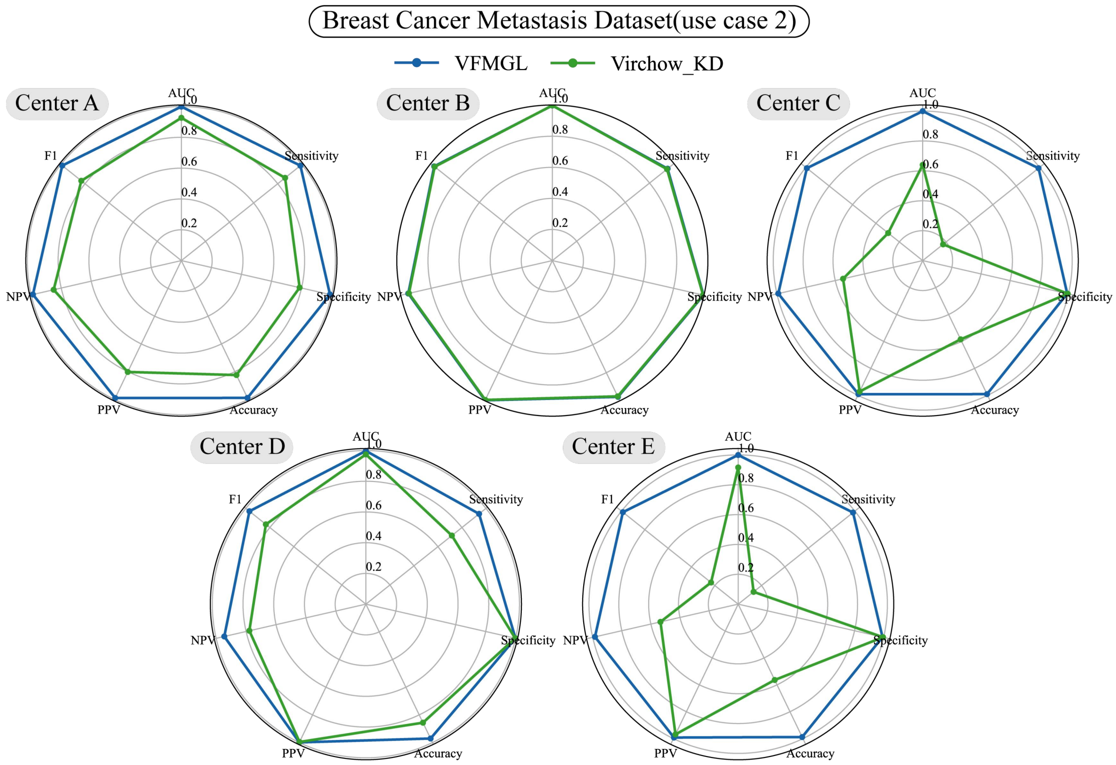


**Supplementary Fig.12 Performance comparison between VFMGL and Logit-based Knowledge Distillation in use case 2.** Notes: AUC, Area Under the Curve; PPV, Positive Predictive Value; NPV, Negative Predictive Value; VFMGL, Vision Foundation Model General Lightweight; KD, Knowledge Distillation. Logit-based Knowledge Distillation (KD) helps the student model achieve better generalization in classification tasks by aligning its probability distribution predictions with those of the teacher model, usually requiring the student and teacher models to share the same label space. To compare the performance of VFMGL with the logit-based KD method on multi-center medical data, we used Virchow and ResNet18 as the teacher and student models, respectively, for the logit-based KD method. The Virchow model, based on the DINOv2 framework, was pre-trained on 1.5 million whole-slide histopathology images (including breast cancer pathology images) and then used model embeddings and nearly 80,000 annotated medical samples to build a classifier for specific downstream tasks. Therefore, in the breast cancer pathology image classification task (use case 2), we compared VFMGL with the logit-based KD method (Fig. S12). The results indicate that VFMGL achieved higher scores across multiple metrics on multi-center data, with stable predictive performance. Further details of the results are provided in Supplementary Table 16. Source data are provided as a Source Data file.

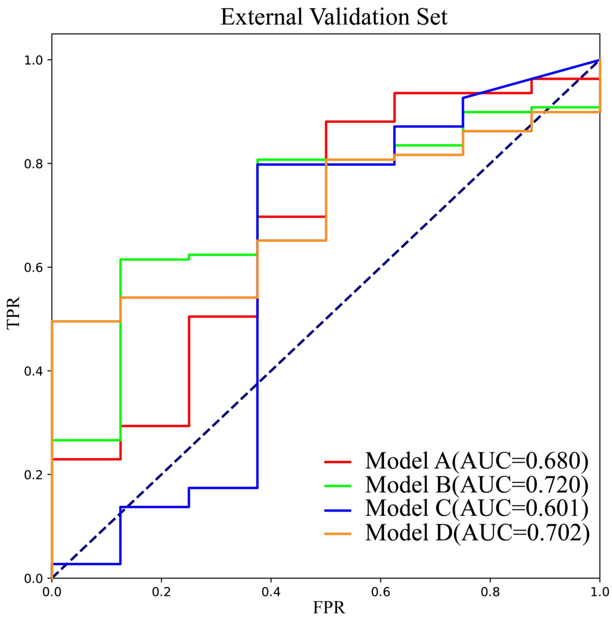


**Supplementary Fig.13 The ROC curves for VFMGL on external center F is shown.** Notes: ROC, Receiver Operating Characteristic curve; AUC, Area Under the Curve; TPR, True Positive Rate; FPR, False Positive Rate. Source data are provided as a Source Data file.

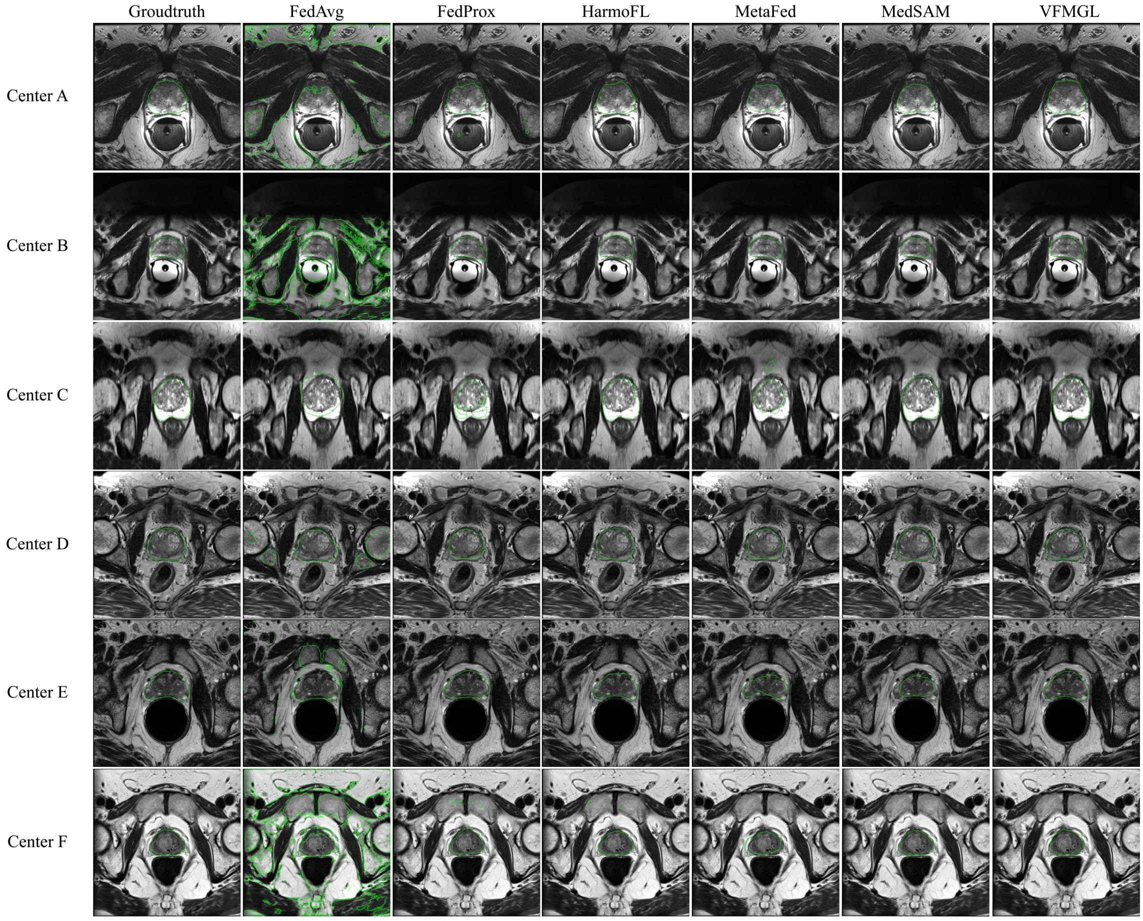


**Supplementary Fig.14 The segmentation results of the prostate along with comparisons.** Rows 1-6 depict examples from Centers A-F respectively, where the first column represents the ground truth labels, and columns 2-7 represent the segmentation results of each method. Notes: VFMGL, Vision Foundation Model General Lightweight.

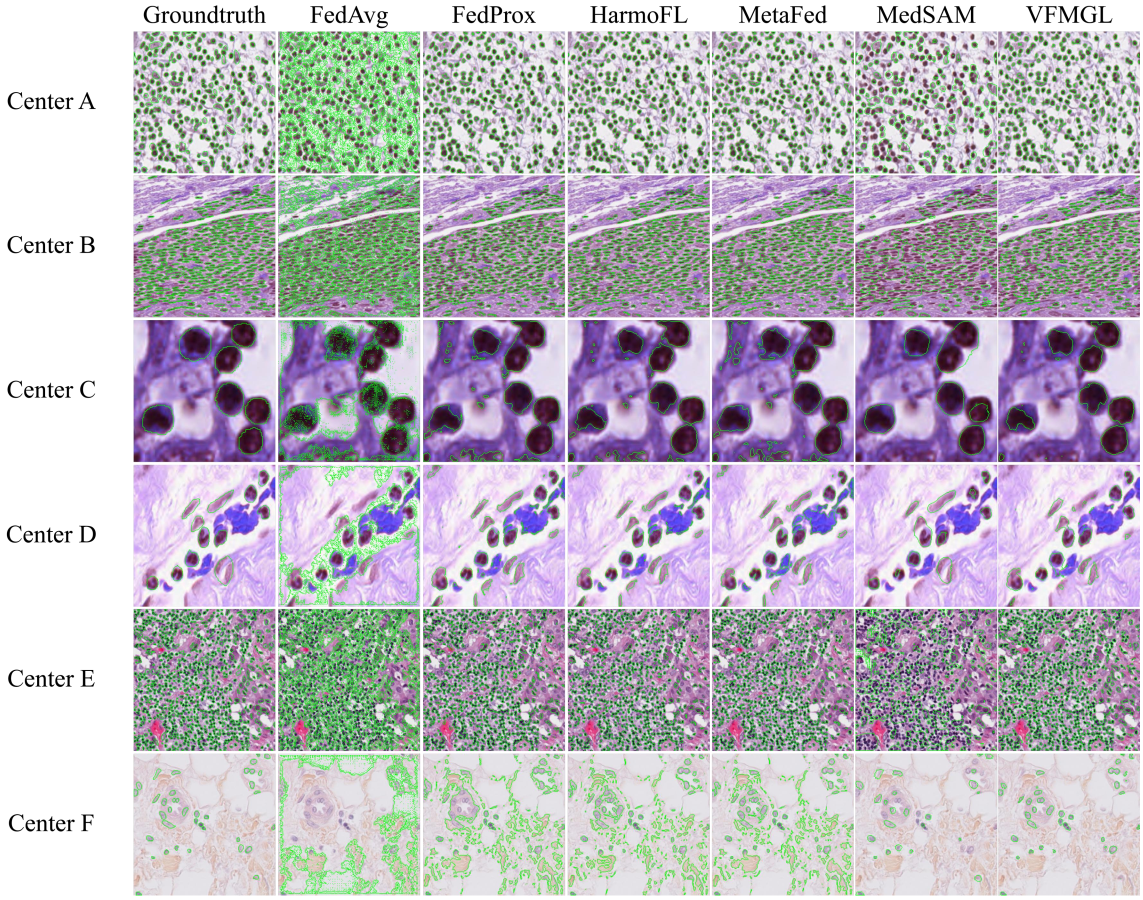


**Supplementary Fig.15 The segmentation results of the cell nuclei along with comparisons.** Rows 1-6 depict examples from Centers A-F respectively, where the first column represents the ground truth labels, and columns 2-7 represent the segmentation results of each method. Notes: VFMGL, Vision Foundation Model General Lightweight.

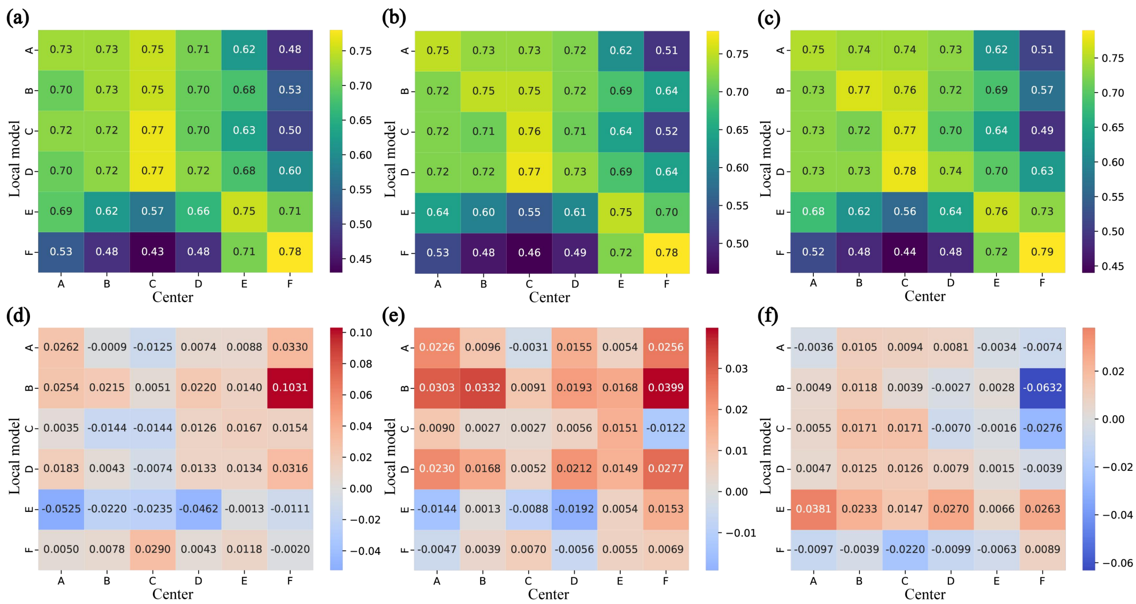


**Supplementary Fig.16 Ablation experiments of VFMGL in use case 4. (a)** Performance when constructing models using only the HGKT method. **(b)** Performance when constructing models using only the HGKT+KD method. **(c)** Performance when constructing models using the HGKT+KD+DDBL method. **(d)** Models performance change from subfigure (a) to (b). **(e)** Models performance change from subfigure (a) to (c). **(f)** Models performance change from subfigure (b) to (c). Notes: HGKT, Heterogeneous-model General Knowledge Transfer; KD, Knowledge Distillation; DDBL, Data Deduction in Batch Level. Source data are provided as a Source Data file.

## Supplementary References

1. Luo, J., Vong, C.-M. & Wong, P.-K. Sparse Bayesian extreme learning machine for multi-classification. IEEE Trans. Neural Netw. Learn Syst. **25**, 836–843 (2014).